



Space weather-related activities and projects on-going at INAF-Turin Observatory

Alessandro Bemporad¹ · Silvano Fineschi¹ · Lucia Abbo¹ · Carlo Benna¹ · Ruggero Biondo¹ · Gerardo Capobianco¹ · Francesco Carella² · Alberto Cora¹ · Federica Frassati¹ · Silvio Giordano¹ · Hervé Haudemand¹ · Federico Landini¹ · Davide Loreggia¹ · Salvatore Mancuso¹ · Andrea Mignone¹ · Gianalfredo Nicolini¹ · Maurizio Pancrazzi¹ · Francesco Salvati¹ · Roberto Susino¹ · Daniele Telloni¹ · Luca Zangrilli¹

Received: 2 March 2023 / Accepted: 6 September 2023
© The Author(s) 2023

Abstract

The Solar Physics Group at the INAF-Turin Astrophysical Observatory (OATo) is actually involved in different Space Weather (SW) projects and missions. In particular, this Group is currently providing for the ESA SWESNET portal two new data analysis tools aimed at (1) the automated identification of magnetic flux ropes from the in situ data (CME magnetic effectiveness tool) and (2) the automated identification and arrival prediction of CMEs from remote sensing and in situ data (CME propagation and forecast tool). The Group is also developing numerical tools for future applications of interest for SW under the project SWELTO-Space WEather Laboratory in Turin Observatory. Moreover, the Group is participating in two SW missions, and in particular in Helianthus (research and development project on solar photonic propulsion for early SW warnings) and Selene (Solar Exploration by Lunar Eclipsing with Nanosatellites Experiment). In addition to this, the Group is leading or is involved in other “SW enabling science” projects, and in particular the Metis coronagraph on-board ESA Solar Orbiter mission, the ASPIICS coronagraph on-board ESA PROBA-3 mission, and the CorMag coronagraph on-board HEMERA stratospheric balloon. In this framework, the OATo Solar Physics Group is working on fundamental research on “SW enabling science”, dealing with the origin and acceleration of solar wind and Coronal Mass Ejections with remote-sensing data, and their interplanetary propagation and evolution with in situ data.

Keywords Space weather · Image processing · Automated tools · Forecasting · Geomagnetic storms

1 Introduction

According to the definition of Space Weather (SW) provided by the European Space Agency (ESA), “Space weather is the physical and phenomenological state of natural space environments. The associated discipline aims, through

observation, monitoring, analysis and modeling, at understanding and predicting the state of the Sun, the interplanetary and planetary environments, and the solar and non-solar-driven perturbations that affect them, and also at forecasting and nowcasting the potential impacts on biological and technological systems” (Lilensten et al. 2008). This complete definition already exemplifies the key challenges that must be addressed to aid the development of a SW program.

The first step is of course related to our physical understanding of phenomena responsible for SW effects. In principle, a forecasting service could be developed even without a real physical understanding of the involved processes, based for instance on a statistical approach or most recent machine learning methods. Nevertheless, these kinds of approaches are reasonable the more the involved processes have common origins and also common developments. Unfortunately, this is not the case for SW events: the chain of events leading

This paper belongs to the Topical collection “Frontiers in Italian studies on Space Weather and Space Climate”, that includes papers written on the occasion of the Second National Congress of SWICo, “Space Weather Italian Community”, held on February 9–11 2022 in Rome at ASI, “Agenzia Spaziale Italiana”.

✉ Alessandro Bemporad
alessandro.bemporad@inaf.it

¹ Turin Astrophysical Observatory, INAF, via Osservatorio 20, 10025 Pino Torinese, TO, Italy

² Dipartimento di Fisica, Università di Torino, via Pietro Giuria 1, 10125 Turin, TO, Italy

to the same phenomenon (e.g., interplanetary shocks accelerating particles, energetic particles impacting the Earth's magnetosphere, ionospheric disturbances leading to radio scintillations, etc.) can be totally different for different events (see the recent review by Buzulukova and Tsurutani 2022).

A forecasting of SW events requires not only a better understanding of the sources on the Sun (e.g., what triggers solar flares and eruptions), but also a better understanding of how different astrophysical systems (solar corona, interplanetary space, Earth's magnetosphere, ionosphere and atmosphere) respond to the energy input coming from the source in the previous step following the cause–effect Sun-to-Earth chain reaction. Also, even just the monitoring of SW conditions requires very different instruments observing radiation from the X-rays to the radio-bands, and particles in different energy ranges, and these instruments need to be deployed in very different environments, such as interplanetary space, near-Earth magnetospheric space, and also on the ground. For these reasons, it is important at the same time to improve our physical understanding of SW phenomena, to develop new numerical models and tools, and also to develop and deploy new instruments.

The Solar Physics Group at the INAF-Turin Astrophysical Observatory (INAF-OATo) has been carrying out for several years various activities to contribute to the above topics. This paper summarizes these activities and is divided into the following three main parts:

- a description of the projects currently going on at INAF-OATo aimed at the provision of SW services (Sect. 2),
- a summary of other projects that are not directly aimed at the provision of SW services but can be considered as SW enabling science ones (Sect. 3),
- a quick summary of the main research topics carried out in INAF-OATo and related with SW as enabling science research (Sect. 4).

All these activities give relevant contributions to the current efforts going on in Italy to provide SW capabilities at the national level, as summarized by Plainaki et al. (2020).

2 Space weather projects

2.1 Heliospheric space weather initiatives-HelioMeteo

In the field of the Heliospheric Space Weather, OATo is leading a set of initiatives—referred to as “HelioMeteo” for short—in collaboration with other INAF institutes, universities and industries. The HelioMeteo projects are: “Space It Up”, funded by the Italian Space Agency (ASI), SWESNET funded by the European Space Agency (ESA),

and Alxtreme, funded by the Italian Government's Foundation “Cassa Depositi e Prestiti”.

2.1.1 SWESNET

The ESA SWESNET program (Space Weather Service Network Development and Pre-Operation Part 1) addresses SW service users in different domains (S/C design, operations, Space Surveillance & Tracking (SST) services, power systems operators, radio link services, airline aerospace, auroral tourism, etc.). Data and products are provided through a network of five Expert Service Centres. Each of these comprises a set of Expert Groups contributing with particular data, products and/or expertise. Solar Weather Expert Service Centre (S-ESC) INAF contributor is the Catania Astrophysical Observatory, while OATo is contributing to the Heliospheric Expert Service Centre (H-ESC). The OATo contribution, consisting in two SW tools dealing with the detection with remote-sensing and in situ data of Coronal Mass Ejections (CMEs), is quickly described below:

- **CME magnetic effectiveness tool**

The CME magnetic effectiveness tool (Telloni et al. 2019) is aimed at the automated detection of magnetic flux ropes in the Lagrangian point L1 based on the analysis of in situ data. The automated detection is based on the quantification of the so-called “magnetic helicity” H_m defined as

$$H_m = \int_V \mathbf{A} \cdot \mathbf{B} dV \quad (1)$$

where \mathbf{B} and \mathbf{A} are, respectively, the magnetic field and the magnetic vector potential in the considered plasma volume V . The magnetic helicity can be interpreted as a measurement of the amount of twist, linkage, and whirl in magnetic flux tubes in a closed volume (Dasso 2009), and is considered as an intrinsic property of CMEs and embedded flux ropes. In this regard, CMEs can be considered as “one of the means by which the Sun ejects magnetic helicity excess into the interplanetary space” (Chandra et al. 2010), helicity being accumulated in its interiors during the solar cycle.

More in detail, the tool developed for the SWESNET program is based on the original idea proposed by Telloni et al. (2012) using the wavelet transform applied to sequences of in situ data to investigate the time behavior at different scales of reduced magnetic helicity $H_m^{(r)}$ given by

$$H_m^{(r)}(k, t) = \frac{2 \operatorname{Im}[\tilde{\mathbf{B}}_y^*(k, t) \cdot \tilde{\mathbf{B}}_z^*(k, t)]}{k} \quad (2)$$

where $\tilde{B}_y^*(k, t)$ and $\tilde{B}_z^*(k, t)$ are the wavelet transforms of the y and z magnetic field components, and k is the wave-number in the sunward direction. The above definition is thus employed in the tool to quantify the helicity content of the ICMEs crossing the spacecraft. Since the helicity associated with the large-scale structure of Parker’s spiral is dominant over the contribution due to ICMEs, the magnetic helicity spectrum is compensated to account for the 8/3 background scaling. This procedure (described in details in Telloni et al. 2012, 2013, 2019) allows the smaller-scale helical structures to emerge.

More than that, the algorithm can quantify the capability of the detected ICMEs of inducing geomagnetic storms on Earth. This can be done (as described in Telloni et al. 2019) based on the measurement of the kinetic E_k and magnetic E_m energies embedded in the flux rope, after compensation for the background solar wind speed and magnetic field fluctuations. A threshold on the measured values for E_k and E_m can be optimized also according to the observed occurrence of geomagnetic storms based on the value of the so-called “disturbance storm time” (Dst) index, mostly representative of additional components of the geomagnetic field induced by the intensification of the ring currents (e.g., Hamilton et al. 1988). This was done by testing the period between

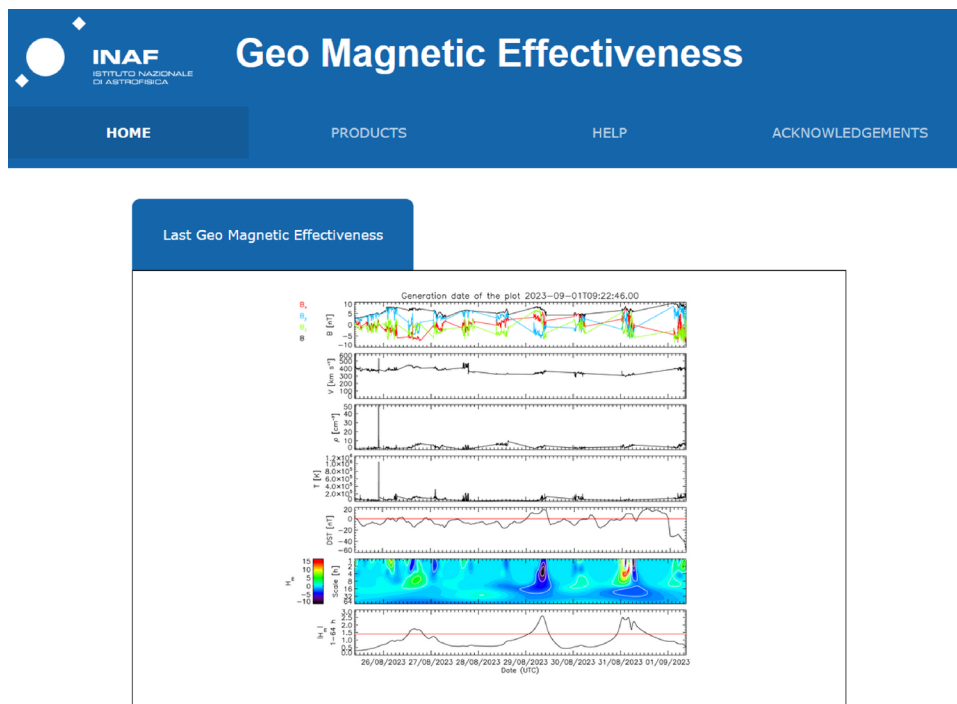
2005 and 2016, thus almost completely spanning solar cycle 24. Results obtained after this testing campaign show that this tool predicts, with an efficiency of 86%, any geomagnetic disturbance associated with a decrease of the Dst-index below -50 nT (see, Telloni et al. 2019, for more details). An example of output product is shown in Fig. 1.

• **CME propagation prediction tool**

The main goal of the CME propagation prediction tool, which is going to be integrated into the ESA SWE portal, is to provide an early warning related to CMEs, which are among the most powerful phenomena that occur within our Solar System and can severely impact on human activities in space and on the ground. The tool consists of several algorithms that take in input white-light coronagraphic data obtained almost in real-time by the suite of LASCO coronagraphs onboard the SOHO spacecraft and in situ plasma measurements from the probes STEREO-A, orbiting the Sun, and the Deep Space Climate Observatory (DSCOVR), located at the Lagrangian point L1. The algorithms have the following tasks:

- automated detection of halo/partial-halo CMEs in LASCO/C2-C3 images,

Fig. 1 An example of output product provided by the CME magnetic effectiveness tool



This web page forms part of the European Space Agency’s network of space weather services and service development activities, and is supported under ESA contract number 4000134036/21/D/MRP. For further product-related information or enquiries contact helpdesk. E-mail: helpdesk.swe@esa.int All publications and presentations using data obtained from this site should acknowledge INAF, ALTEC and The ESA Space Safety Programme. For further information about space weather in the ESA Space Safety Programme see www.esa.int/spaceweather Access the ESA SWE Portal here: <https://swe.ssa.esa.int>.



- automated identification of the CME features and derivation of its geometrical and dynamical parameters through geometrical modeling,
- computation of an interplanetary (IP) model of the ecliptic solar wind,
- modeling of the CME propagation in the IP space and estimate of the arrival time at Earth.

The detection of a CME appearing in the coronagraph field of view is performed by employing a modified version of the CME detection algorithm implemented by the Solar Orbiter/Metis instrument (see Sect. 3.1), which is based on the analysis of the difference of two consecutive images acquired by the same telescope. The algorithm is able to distinguish halo/partial-halo CMEs (that could potentially propagate toward Earth) from other CMEs that will not affect our planet (which are therefore ignored). Detection of an event is the trigger for all subsequent actions.

As the CME leading edge is identified in the coronagraphic images, its shape is modeled with the Elliptic Cone Model (see Zhao et al. 2002), which is a very simple geometrical model but proved to be efficient enough for halo/partial-halo CMEs. The elliptical fit to the CME front allows for the determination of the real angular extension of the CME, the propagation direction (defined by the Stonyhurst coordinates of the cone axis), and the true radial component of the CME speed. An estimate of the total mass of the CME is also obtained, using the method described by Vourlidas et al. (2000).

All CME parameters are then used to numerically solve the analytical equation of motion provided by the 2D Drag-Based propagation Model (DBM; see Vršnak et al. 2013), which relies on the assumption that the dynamics of CMEs in the IP are governed by the magneto-hydrodynamic (MHD) drag force originating between the CMEs and the ambient solar wind.

The solar-wind speed and density which are input to the DBM are retrieved from a semi-empirical model of the ecliptic IP solar wind that is obtained by another algorithm of the tool, by combining in situ plasma measurements with the analytical model of the IP magnetic field structure by Parker (1958). The model covers all distances from the Sun to the Earth on an angular sector centered on the Sun–Earth line and therefore allows for simulation of the propagation of the 2D front of the CME and its deformation due to the different wind speeds along different wind streams.

The simulation is used to provide a prediction of the arrival time of the CME front at the Lagrangian point L1, as well as its final speed, which controls to a large degree the strength of the CME interaction with the

terrestrial environment. An example of output product is shown in Fig. 2.

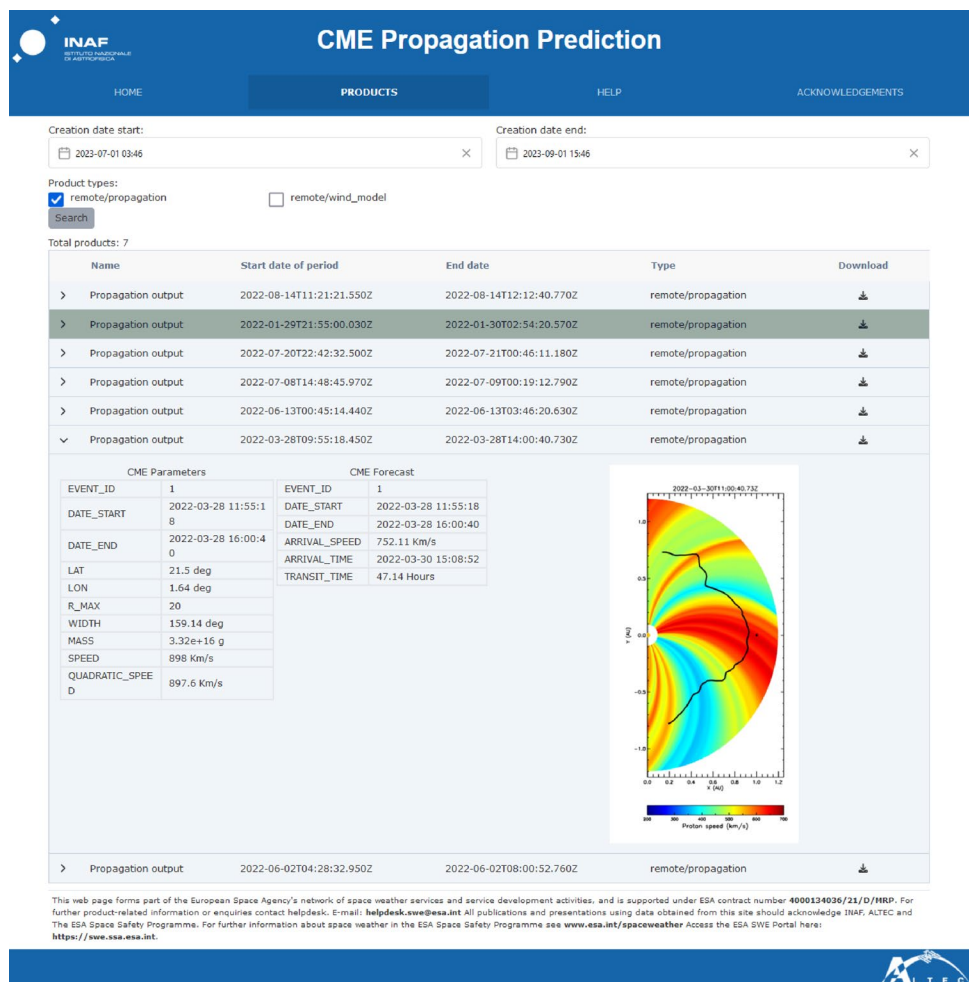
2.1.2 Space It Up

Within the framework of the Next Generation EU program, a national consortium including 13 Universities, 10 Research Institutes and Centers, and 10 Space Industries proposed to ASI the realization of the “SPACE IT UP” research and technology hub to address the major challenges concerning the mankind’s space domination for both downstream and upstream applications. One of the SPACE IT UP spokes will be entirely devoted to the protection of critical infrastructures and space exploration from SW threats, and will foster synergies on SW national activities between academy, industry, and research centers in such a way to significantly impact the Italian space sector on SW starting in 2023 and for the next three years. OATo leads the INAF responsibility of this SW Spoke (see Fig. 3).

This Spoke is aimed at protecting critical infrastructures from SW events by fostering research and tools that can potentially be translated into future operational services. The main objectives are: (1) carry out novel scientific research to advance our understanding of the origin and evolution of SW phenomena from the Sun to the Earth, also enabling future SW services; (2) evaluate the SW effects on ground and space-based infrastructures; (3) advance the capability to monitor and forecast SW threats in a timely manner to ensure effective mitigation for the protection of the planet; (4) design innovative space architectures and technologies to make a quality leap in prevention and mitigation of SW effects.

Some expected results are: (1) development/refinement of modeling capabilities and advanced data analyses able to interpret a broad range of observations of the Sun–Earth system and unveil the origin of SW drivers in the solar atmosphere, solar wind and solar energetic particles generation and transport, and solar wind—magnetosphere–ionosphere coupling; (2) assessment of particle radiation environment; (3) development and/or validation of novel SW forecasting tools in the whole Sun–Earth connection chain, including AI-based analyses; (4) identification of effective real-time proxies that can be provided by monitoring instruments, both in space and on the ground, and preparation for their integration into an Alert Network; (5) assessment of SW effects on near-Earth and ground-based infrastructures; (6) requirements definition of a network that can respond quickly and efficiently to the forecasts of SW events, both for terrestrial and space-based infrastructures. (7) definition of the scientific and technological requirements and design of new missions architectures, including spacecraft/satellite

Fig. 2 An example of output product provided by the CME propagation prediction tool



specification and space instrumentation definition aimed at spatially and temporally resolved forecasting of SW events.

Impact on the economic, scientific, social, and cultural system will provide significant progress in understanding the origin and evolution of SW phenomena, as well as novel modeling and specific applications for SW forecasting in the whole Sun–Earth connection chain. A noticeable impact will be to uncover new knowledge and expand technology developed to reach the main objectives of the project. The innovative technologies in the fields of AI and space instrumentation developed for SW operations will also have applications in other fields (e.g., big data, optical sensors) with a relevant economic impact. The obtained results will be useful to provide important constraints for the safety of the future missions dedicated to human space exploration.

2.1.3 Alxtreme

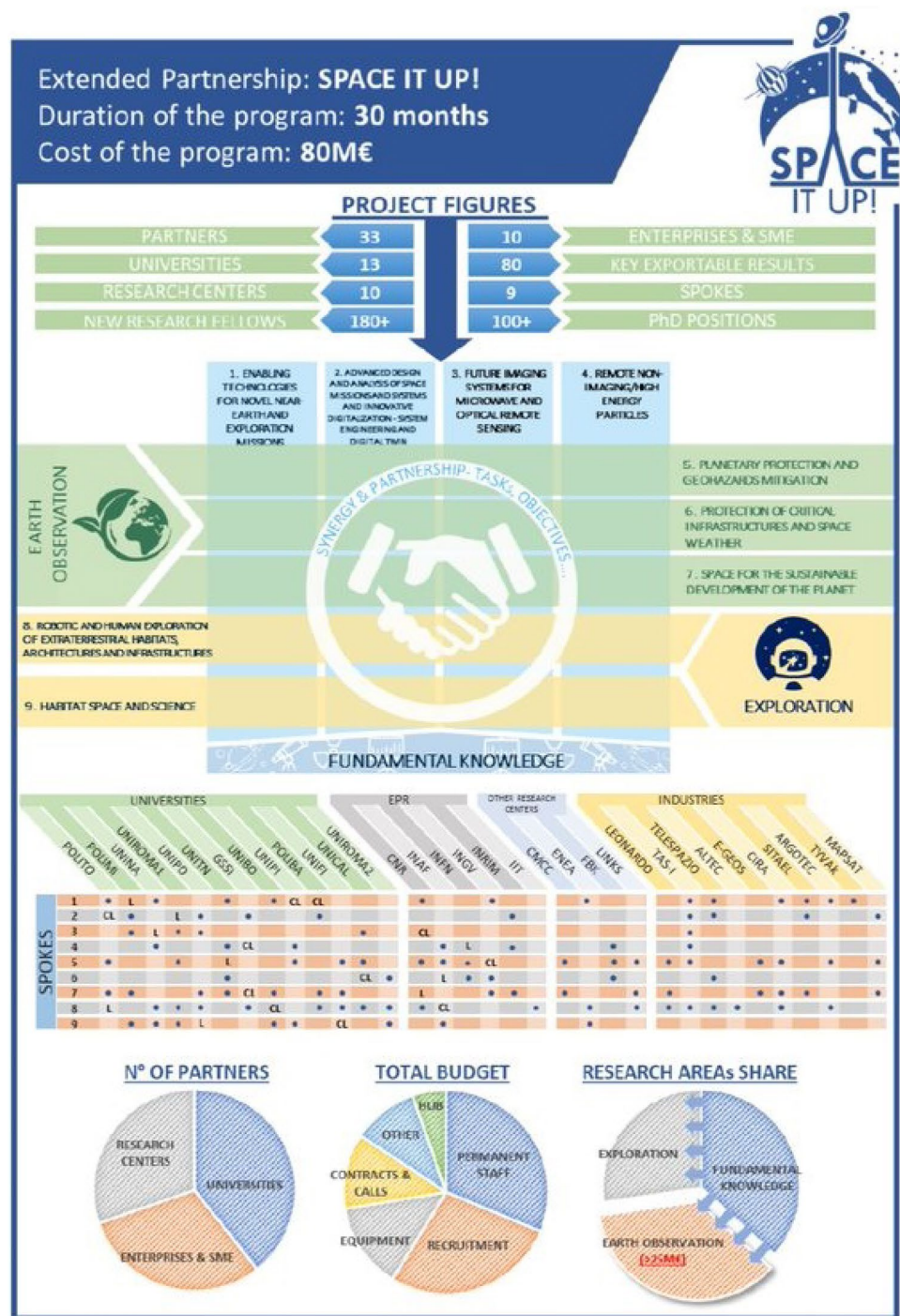
OATo collaborates in Alxtreme: Physics-based Artificial Intelligence (AI) for predicting extreme weather and SW events.

The purpose of this collaboration by the University of Genova is the development of a pilot project that uses AI in the field of Environment and the green transition. The Project intends to build a pipeline able to calibrate (1) numerical models based on the physics of SW, with the aim of protecting satellite infrastructures designed first for environmental and meteorological monitoring, and for other potential applications; and (2) numerical models based on the physics of the atmosphere, with the aim of anticipating the occurrence of extreme weather events and supporting decisions of civil protection agencies and other Institutions.

On a technical level, this project intends to integrate the most innovative machine and deep learning techniques with numerical models to simulate highly complex dynamical systems. On a strategic level, the involvement of territorial partners with notable experience in applied research, technology transfer, and territorial protection, will ensure systematic validation and a level of dissemination of the project results aimed to enhancing Alxtreme technological and social impacts.

Specifically, OATo will contribute with the knowledge of Solar Physics, in particular propagation models

Fig. 3 Infographic summarizing the Space It Up “hub” comprising 9 lines of research—“Spokes”. OATo leads INAF responsibility for the “Spoke” Space Weather (#6 in the diagram)



of eruptive events and corresponding numerical tools for their simulation. The models will be validated by accessing currently acquired data from Solar Orbiter/Metis and ASPIICS/PROBA-3, SOHO/LASCO, Stereo and DISCOVR, and archived data from SOHO/UVCS.

2.2 SWELTO

SWELTO (Space WEather Lab in Turin Observatory) (Bemporad et al. 2021) is a multi-purpose SW project aimed mainly at: (1) the development of new tools for future

applications of interest for SW, (2) the deployment of new sensors, or the employment of existing sensors for possible future SW applications, and (3) the outreach of SW topics to the general public. These three main targets are briefly explained below:

2.2.1 New tools development

Within the SWELTO project, new ideas for the provision of future SW tools are tested and implemented. Each new tool is provided in a first version already working in real time on a local Workstation. With respect to what was originally described in Bemporad et al. (2021), some of the already existing tools are currently being upgraded. In particular, with respect to what is already described in Bemporad et al. (2021), the “SunNow module” (aimed at the monitoring of real-time conditions on the Sun) has been upgraded to also provide in real time the distribution of photospheric magnetic fields as measured by SDO/HMI. This module is of fundamental importance also for the execution of the “EUV monitor module” (now providing daily maps of the Sun automatically clusterized to identify coronal holes and active regions), and for the production of monthly SW bulletin videos (see later). The “In Situ module” (aimed at the monitoring of real-time conditions in the interplanetary space) has been upgraded to provide a totally new visualization of the *in situ* data measurements not only in the classical version of a time plot, but also in a much more attractive display in the format of a classic speedometer (Fig. 4). The GIF animation (created automatically everyday) shows the evolution over the last 24 h of 3 solar wind plasma parameters measured in the Lagrangian point L1: the plasma density, velocity, and temperature. This animation is now also provided as an outreach product for the “Sorvegliati Spaziali” (“space surveillance”) portal.

The “Parker Spiral module” (aimed at the real-time reconstruction of the distribution of plasma densities and velocities in the interplanetary space) has also been upgraded,

particularly to better take into account some numerical problems affecting in a few cases the numerical reconstructions. Moreover, now this module provides an animation showing the shape of the Parker spiral as reconstructed over the last few days. The download of the photospheric field measurements from HMI is also aimed at the commissioning of the “EUV monitor module” for the automatic identification of structures of the Sun based on EUV images and photospheric magnetograms, utilizing an FCM (Fuzzy C-Means) algorithm (Carella and Bemporad 2020). An upgraded version of this tool is also under development to provide better identification of coronal hole regions. The “CorDens module” is also now being upgraded to extend the automated density measurements from LASCO C2 data at all latitudes to include the polar regions. The aim of this extension is to provide extended boundary conditions to run a 3D version of the “Parker Spiral module” also currently under development. All the results from the tools are made available in real-time through the SWELTO portal.

2.2.2 New sensors deployment

SID monitor antenna The detection of sudden ionospheric disturbances (SIDs) with a radio antenna is interesting not so much for possible research purposes that are quite limited, but rather for possible monitoring of the Ionospheric state, educational workshops and dissemination events with the public and with schools.

The already existing antenna for the identification of the SID events (“SIDmonitor module”) has been upgraded building a new radio antenna with a 200m long cable rolled-up over a hexagonal perimeter by 4.5m covering one area of about 1.46 m² (Fig. 5, left panel). This active antenna, now installed in the attic of the Observatory, has been connected to the SuperSID monitor procured from Stanford Solar Center (see Bemporad et al. 2021, for more details).

Thanks to the increase in the cable length and also in the covered area, the S/N ratio has now significantly

Fig. 4 The new version of the “InSitu Module” providing in real-time the latest 24h measurements of solar wind density (left), velocity (middle) and temperature (right)

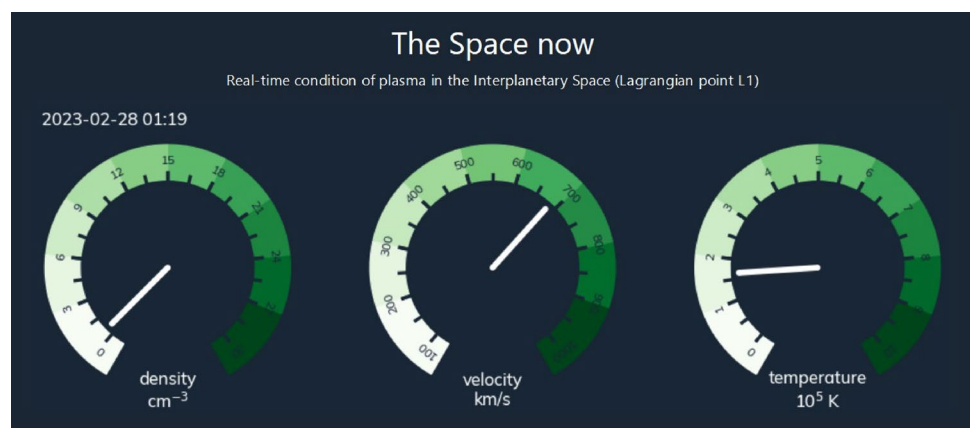
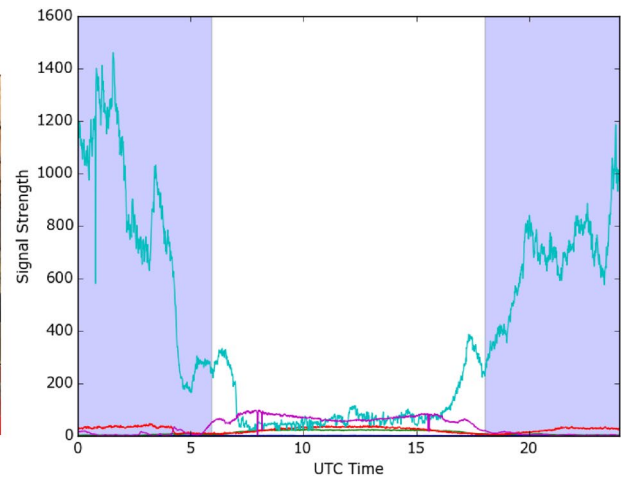


Fig. 5 The new antenna for the “SIDmonitor module” (left) and an example of acquisition on April 21, 2021 (right). Different curves in the right panels show different frequency bands (see text)



increased (Fig. 5, left panel) allowing the detection of a clear day–night ionospheric modulation. In particular, the strongest signal is detected in two frequency bands centered around 21.75 kHz (corresponding to the HWU facility transmitter located in Rosnay, France) and at 23.4 kHz (corresponding to the DHO38 facility transmitter located near Rhaudefehn, Saterland, Germany). Unfortunately, due to a lightning strike that struck the Observatory building in the end of 2022, this antenna has been temporarily dismantled, and it will be put back into operation as soon as all electric systems in the Observatory have returned to their nominal state.

Fluxgate magnetometer The evidence of the effects of solar flares events on the geomagnetic field was given for the first time by Mr. R.C. Carrington in 1859, who observed the solar event of September 1, 1859 and correlated it with simultaneously occurred sudden jump of the three geomagnetic elements recorded at Kew Observatory (Carrington 1859). As a result of the increase of the total amount of radiation occurring during solar flare events, fast variation of the geomagnetic field is observable. For that reason, local measurement of the geomagnetic field is a good marker of solar activity and of interest to the SW.

The expected geomagnetic field provided by the World Magnetic Model (WMM) for our observing site (i.e., Pino Torinese, ITALY) is:

- North–South component: 22872.8 nT;
- East–West component: 1206.8 nT;
- Vertical component: 41571.7 nT

with annual variations of:

- North–South: 9 nT per year;
- East–West: 62 nT per year;
- Vertical: 52 nT per year.

A geomagnetic field map for the latitude range 30°–75° N and longitude 15° W–45° E at is shown in Fig. 6. The plot is based on current World Magnetic Model (WMM) and the data provided by the NOAA/NCEI.

A fluxgate magnetometer has been procured (see also Bemporad et al. 2021) in order to provide an estimate of these components. The main characteristics of the magnetometer are summarized in Table 1. The magnetometer outputs are connected to a USB-controlled 24-bit ADC (Analog to Digital Converter) also procured for SWELTO. With this configuration, the performances reported in Table 2 are expected.

Functional test campaigns have been performed in December 2020 and May 2021. During the last test campaign, the in-house developed acquisition software has been used. The results show a good agreement between the expected performances and the measurements. A 50 Hz component was present in the measurements. The use of shielded cables combined with the use of a low-pass filter will fix this problem. As example, the power spectral density (PSD) for one channel is depicted in Fig. 7. The 50 Hz component is clearly visible. In the next future (after all the electric problems related to the lightning strike mentioned above are solved), the magnetometer will be installed in the wood nearby the Observatory to start monitoring the geomagnetic field.

2.2.3 SW outreach and bulletins

After a period of tests and experiments based on the creation of weekly SW reports, in April 2022, we began a collaboration with the INAF Educational project called “*Sorvegliati Spaziali*” (“space surveillance”) to provide monthly bulletins. The experimental edition was released on the “*SWELTO TV*” YouTube channel. In this test phase, we

Fig. 6 WMM map of the geo-magnetic field (total intensity)

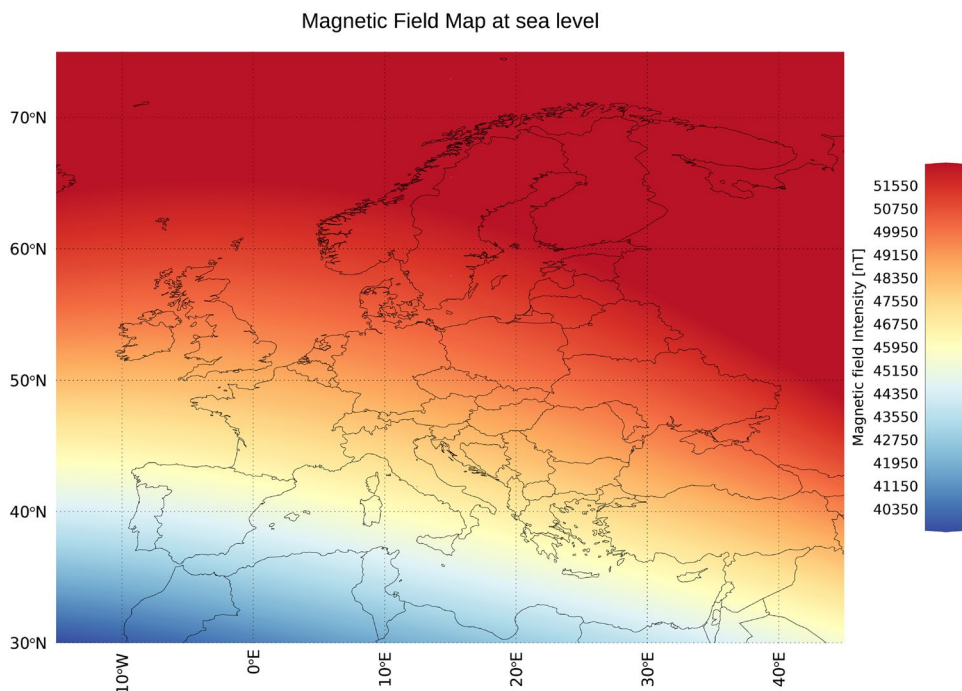


Table 1 Main characteristics of the fluxgate magnetometer procured for SWELTO (see text)

Characteristic	Value
Channels	3 + 1 (temperature)
Magnetic field range	±60 μT
Operational temperature range	- 40 to + 70 °C
Scaling factor	166 mV/μT
Offset temperature coeff.	±0.3 nT/°C

Table 2 Expected performances of the fluxgate magnetometer procured for SWELTO (see text)

Performance	Value
Resolution	7 pT
Accuracy	< 15 pT (after calibration)
Sampling frequency	10 Hz

posted 12 videos with a duration of 3–7 min regarding the observed solar activity during different phases of the solar cycle, achieving an average of 90 views each.

The new series of monthly SW bulletins entitled “Che Sole che fa” is now published on the “[Sorvegliati Spaziali](#)” website (see Fig. 8) and reposted by MEDIAINAF TV, the institutional YouTube channel with more than 46,000 subscribers. The news about the SWELTO bulletins was also broadcast on TV by TG Leonardo, the national science and

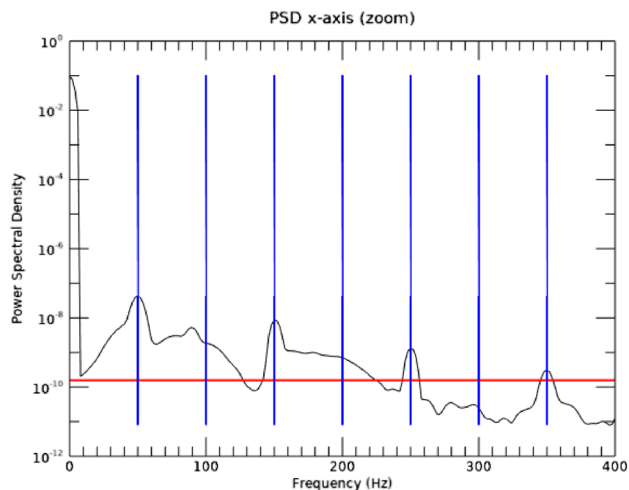


Fig. 7 Example of power spectral density for x-channel (limited to 400 Hz). Measurements of December 2020. Sampling frequency of 4096 Hz

environment newscast. At the time of writing, we published 15 monthly videos starting from April 2022, achieving a total of 21,750 views, an average of 1450 views for each video, and a peak of 3836 views for a single video.

2.3 Helianthus

Helianthus is a technological development program funded by the Italian Space Agency for a Phase A study of a SW station with solar photonic propulsion. Helianthus is designed



Fig. 8 Examples of screenshots from the monthly SW bulletins published on the “Sorvegliati Spaziali” website

to have a synchronous orbit positioned at about 7 million km from Earth toward the Sun, thus much closer to the Sun with respect to historical SW instrumentation, which is typically orbiting the Earth or the Sun–Earth L1 at 1.5 million km from Earth. The sub-L1 position (Fig. 9) guarantees an earlier detection of solar eruptive events of about 1 h in advance with respect to stations positioned in L1 or in geostationary orbits. The mission PI is Prof. C. Circi of Università di Roma La Sapienza. INAF is responsible for the definition of the strawman scientific payload.

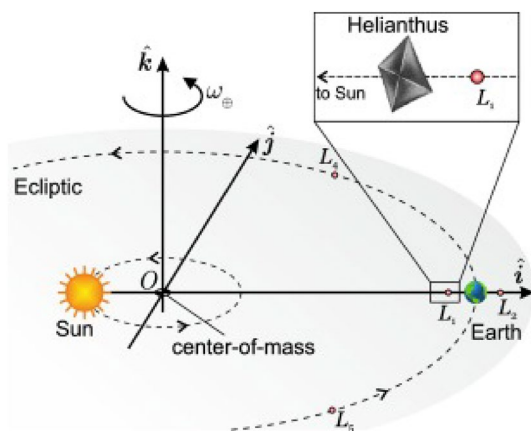


Fig. 9 A sketch of the orbital geometric configuration allowing monitoring of interplanetary medium closer to the Sun with respect to the Lagrangian point L1—thanks to the photonic propulsion (adapted from Boni et al. 2023)

The scientific payload will be hosted at the center of a 40 m wide sail and will comprise:

- Remote-sensing instruments: an X-ray diode detector to detect Solar Flares and SailCor, a compact coronagraph with a wide field of view (FOV).
- In situ instruments: a plasma analyzer and a magnetometer.

The peculiarity of a sailcraft imposes severe constraints on the dimension and weight of the payload. The payload overall mass shall not exceed 5 kg.

Both the X-ray detector and the in situ instruments have a flight heritage (technological readiness level—TRL: 8–9) and are matching the mission constraints in terms of volume and weight. The magnetometer has been developed by NASA GSFC and basically is a simple RL circuit with a working principle similar to a fluxgate. The plasma analyzer is borrowed from the one developed by NOAA/NASA and has a strong heritage based upon the Rosetta mission (instrument RPC/IES) (Burch et al. 2007). The X-ray spectrometer is a single-diode Amptek XR100FASTSDD, which has a flight heritage but has nevertheless been tested in the laboratory in order to guarantee the suitability of its performance for flare monitoring purposes. The laboratory activity has been run at the XACT (X-ray astronomy calibration and testing) INAF laboratory in Palermo. The only instrument that needed a development matching the mission constraints is SailCor, the wide FOV coronagraph selected for Helianthus.

A coronagraph aims at observing the solar corona, a mean that in the visible is more than 6 orders of magnitude fainter than the photosphere, which is very close in angle. The photospheric light, diffracted by the occulters and scattered by the optics, can easily overwhelm the coronal light on the focal plane. Consequently, particular care shall always be reserved for stray light reduction in designing coronagraphs.

A possibility in constraining mass and dimension, while guaranteeing a low stray light level, is offered by some recent advances in solar coronagraph stray light analysis. A numerical work of Gong and Socker (2004) introduced the concept of the focusing effect induced by the entrance aperture (EA) on the light diffracted by the external occulter. The classical externally occulted coronagraph design foresees three optical stages (Lyot 1932; Evans 1948):

- First stage: an external occulter (EO) positioned in front of the EA of the telescope.
- Second stage: an internal occulter (IO) conjugated to the EO with respect to the primary optics, in order to block the light diffracted by the EO and imaged by the primary optics.
- Third stage: a stop (called Lyot stop) conjugated to the EA, in order to block the light diffracted by the EA and imaged by the primary optics.

By taking advantage of the focusing effect of the EA on the diffraction as simulated by Gong and Socker (2004), the classical Lyot (1932) and Evans (1948) designs of solar coronagraph can be revolutionized. With a suitable optimization of the external occulter geometry and careful positioning of the internal occulter close but before the primary focal plane, the successive stages of the coronagraph can be removed and the detector positioned directly at the primary focal plane. With only one stage, the resulting instrument is considerably shorter and lighter.

A SailCor prototype was designed and manufactured in order to experimentally demonstrate the feasibility of the single-stage coronagraph. The measurements were carried out at the INAF OPSys (Optical Payload System) facility in Torino (Capobianco et al. 2019) in front of a solar divergence simulator. A photo of the setup is shown in Fig. 10. The measurement campaign was extremely successful: for the first time the focusing effect of the EA on the light diffracted from the EO was experimentally proven and the feasibility of a single-stage coronagraph was demonstrated.

2.4 Selene

The Solar Exploration by Lunar Eclipsing with Nanosatellites Experiment (SELENE) is a proposed SW mission with Moon orbiting observatories utilizing lunar limb occultation of the solar disk for detection and propagation prediction

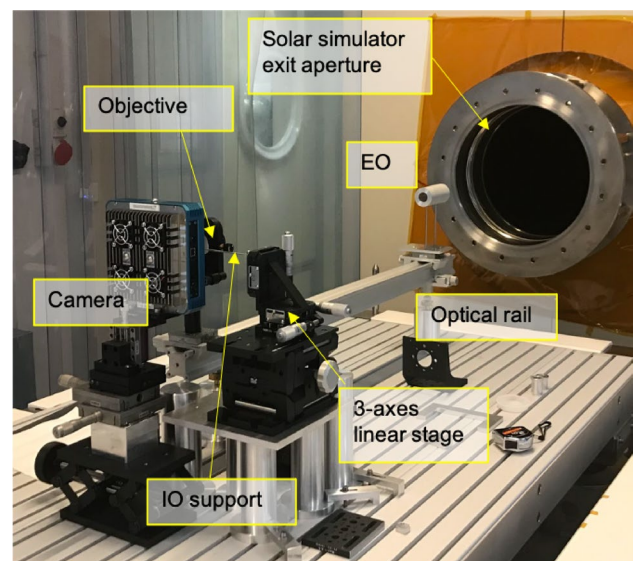


Fig. 10 Picture of the SailCor prototype in front of the solar simulator source at the OPSys facility in Torino

of Earth-directed CMEs. At the same time, SELENE will monitor the heliospheric particle radiation (electron, ions) and magnetic field environment of the Earth–Moon system.

The fastest Earth-directed CMEs can reach our planet in as little as 15–18 h. Slower CMEs can take several days to arrive. Therefore, remote-sensing observations of CMEs provide a valuable early warning of SW-relevant events. Unlike coronagraph telescopes that need complex external and internal occultation systems, in each orbit, the Moon will create a natural eclipse. This greatly simplifies the optical system with respect to classical coronagraphs, and it can fit a small satellite. The SELENE Moon orbiting solar telescope would greatly increase the frequency and duration of solar coronal eclipse observations (hourly to daily) utilizing lunar limb occultation of the solar disk. Near apolune, in the anti-sunward orbit, a simple telescope onboard a cubesat could view fully around the circumference of the lunar dark side the large-scale halo structures associated with CMEs events approaching geospace. In the sunward–perilune orbit, SELENE would be ideal for in situ measurements with field and plasma probes of the upstream solar wind not perturbed by geomagnetic effects. Data time shifts of several days, dependent on solar wind radial speed, would allow a direct correlation between the remotely observed CMEs and the energy distributions of the arriving electrons and ions at the lunar orbit.

The strawman payload would include:

- Coronal Wide-Angle Imager with the wide field-of-view objective and CMOS sensor
- X-ray sensor for solar flares detection
- In situ instrumentation Plasma Analyzer

- Magnetometer

SELENE will be relevant for SW studies and solar activity monitoring also with respect to human presence on the Moon. The “natural eclipse” by the Moon’s occultation of the sun disk has the advantage of providing a FOV coverage of the solar corona that, with the “artificial eclipse” by the classical coronagraphic occulting systems, would take several complex coronagraphs with “nested FoVs” to have. The large dynamic range of the coronal brightness cannot be covered by a single coronagraph due to the far different levels of stray light produced by the diffraction from the different coronagraphs’ over-occultations. More complex coronagraphs, with different “nested” FoVs (e.g., SOHO/LASCO-C1, -C2, -C3 and STEREO/COR1 and COR2) have to be used to image the inner corona (i.e., 1.5–3.0 R_{sun}) and the outer heliosphere (i.e., up to 20–30 R_{sun}). On the other hand, the negligible diffraction from the Moon’s occultation on SELENE allows the Coronal Wide-Angle Camera—which has no occulters—the possibility of imaging the solar corona over a wide range of heliocentric heights, just by changing the exposure times.

In Fig. 11, the insets (a, b) are the images of the same halo CME observed by LASCO-C2 and LASCO-C3, respectively, as it expands. Their “nested” FoVs span from 2 R_{sun} to 6 R_{sun} in LASCO-C2 (a) and from 4 R_{sun} to 30 R_{sun} in LASCO-C3 (b). In inset (b), the FoV of LASCO-C2 is shown scaled to that of LASCO-C3. The insets (c, d) show

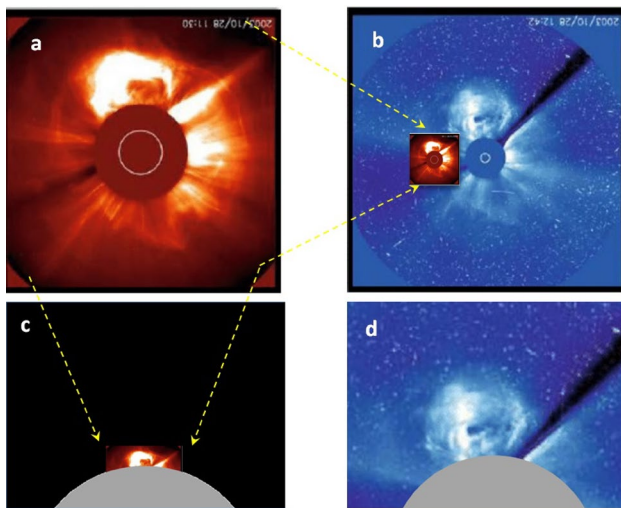


Fig. 11 Panels **a** and **b** are the images of the same halo CME observed by LASCO-C2 and LASCO-C3, respectively, as it expands. Their “nested” FoVs span from 2 R_{sun} to 6 R_{sun} in LASCO-C2 (**a**) and from 4 R_{sun} to 30 R_{sun} in LASCO-C3 (**b**). In panel **b**, the FoV of LASCO-C2 is shown scaled to that of LASCO-C3. Panels **c**, **d** show how the same expanding halo CME would be observed by the Coronal Wide-Angle Camera onboard SELENE orbiting the Moon at its apolune of 10 Moon radii

how the same expanding halo CME would be observed by the Coronal Wide-Angle Camera onboard SELENE orbiting the Moon at its apolune of 10 Moon radii.

3 Space-weather enabling science projects

3.1 Solar orbiter/Metis

Solar orbiter (Müller et al. 2020) is an international collaborative mission between ESA and NASA that will explore the Sun and heliosphere from close up and out of the ecliptic plane, carrying for the first time remote-sensing instrumentation. It was successfully launched on February 10, 2020, from Cape Canaveral (Florida, US) and it is now operating in its nominal mission phase.

The main goal of the Solar Orbiter mission is to address key questions in Solar Physics related to how the Sun creates and controls the heliosphere, and why solar activity changes with time. Addressing these questions will be made possible, thanks to the mission’s unique orbital profile, with a minimum perihelion distance to the Sun of 0.28 AU and an out-of-ecliptic vantage point that will reach $\sim 30^\circ$ heliographic latitude, and its comprehensive suite of in situ and remote-sensing instruments.

Metis (Antonucci et al. 2020; Fineschi et al. 2020) is the coronagraph included in the payload of Solar Orbiter. This innovative instrument, based on the SOHO/UVCS heritage and diagnostic methods, is designed to simultaneously image the full off-limb solar corona between 1.7 and 9 R_{\odot} in both polarized visible light (broad-band between 580–640 nm) and UV H α Lyman- α (121.6 ± 10 nm), at high spatial and temporal resolutions. The annular field of view of the coronagraph can span over a wide range of heliocentric distances depending on the distance of the spacecraft from the Sun.

Metis has been developed specifically to exploit the Doppler-dimming technique to infer the outflow speed of the solar wind, and to address the following scientific objectives in the context of the Solar Orbiter science questions:

- investigation of the coronal regions where the solar wind is accelerated;
- investigation of the regions where the early propagation of CMEs occurs;
- identification and characterization of CME-driven shock fronts accelerating particles in the solar corona;
- study of the global magnetic configuration of the solar corona by the identification of the closed and open magnetic field regions.

The Solar Orbiter mission was not conceived for specific SW applications which crucially depend on the real-time availability of solar and heliospheric data. In fact, due to

the peculiar mission specifications, the data have sometimes long latency in the download, especially when the spacecraft is at a great distance from the Earth. Nevertheless, Solar Orbiter's instruments can allow correlative studies to provide a complete physical description of the plasma involved in the dynamical processes of the solar atmosphere that drive the SW (see Sect. 4).

In particular, Metis observations offer the possibility to map the electron density distribution (through the inversion of the polarized visible light data) and the outflow velocity of the neutral hydrogen/proton component of the solar wind in the corona, providing constraints on the characteristics of the ambient medium in which CMEs and other CME-driven phenomena originate and propagate.

Metis can automatically detect CMEs entering the instrument field of view, thanks to an automated CME detection algorithm implemented on board, which is based on the analysis of the visible light intensity variations in the eight angular sectors 45°-wide that make up the annular FOV (Bemporad et al. 2014). During the out-of-ecliptic phase of the Solar Orbiter mission, Metis will be able to infer the longitudinal distribution of the solar wind streams and CMEs, and single out those potentially affecting the Earth. The properties of the plasma streams and ejections observed by Metis in these cases can provide alternative, essential input to the existing CME propagation models, allowing for their assessment and/or improvement, as well as the development of new ones.

3.2 PROBA-3

PROBA-3, "PROject for On-Board Autonomy", is an ESA mission composed of two spacecraft dedicated to the in-flight demonstration of precise formation flying metrology concept and maneuvers, including formation acquisition, maintenance, resizing and re-targeting. To this end, different metrology instrumentation will be operated to align the two spacecraft down to sub-millimeter accuracy level. When aligned, the two spacecraft (due to launch in July 2024) will realize a giant externally occulted solar coronagraph, with the telescope (named ASPIICS: Association of Spacecraft for Polarimetric and Imaging Investigation of the Corona of the Sun) on one satellite and the external occulter on the other one, at inter-satellite distance of 144 m. The PROBA-3/ASPIICS coronagraph will examine the structure and dynamics of the corona in a crucial region by filling the gap between the typical fields of view of UV-VIS imagers and externally occulted coronagraphs (see Fig. 16).

INAF played an important role within the consortium that realized the ASPIICS coronagraph. In particular, it was the leading institute for the realization, testing, qualification and calibration of the Shadow Position Sensors (SPS), one of the most accurate metrology systems on board of the mission.

The observation of the Sun's Corona in the field of view $[1.1;3.0]R_{\odot}$ plays the role of formation flying validation. Furthermore, the high accuracy expected by the metrology control loop, combined with the mission geometry and location, permits to obtain high spatial and temporal resolution images of the Solar Corona in a region very close to the limb, as never done before.

For this reason, in June 2017, the ESA Science Programme Committee endorsed the mission for additional backing through the Directorate of Science and INAF becomes part of the Science Working Team, as well (Fig. 12).

PROBA-3 will observe the Corona for two orbits per week on average, over a full mission of 2 years, yielding to an improvement of a factor 100 in the duration of uninterrupted observations in comparison with a total eclipse on Earth. The observation will be done throughout 6 spectral channels:

- 1 wide band (5350–5650 Å);
- 3 polarized white light;
- Fe XIV narrow band at 5304 Å;
- He D3 narrow band at 5877 Å.

over a frame of 2048×2048 pixels with a scale of 2.8 arcsec/pixel, with an image cadence of 1 image/2 s, and over a FoV $= [1.098; 3.0] R_{\odot}$. The accurate positioning of the spacecraft with a large separation between the external occulter and the ASPIICS coronagraph permits minimizing the straylight generated by the occulter on the scientific images. This represents the most innovative aspect of making accessible a coronal region very close to the limb of the Sun. Overall, PROBA-3 will permit:

- To observe the transition between closed-field regions (magnetic field dominated) and open-field regions (solar

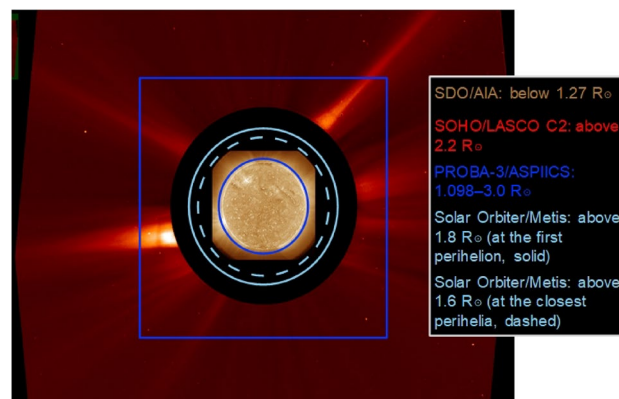


Fig. 12 PROBA-3 FoV compared to solar orbiter

wind dominated) that are poorly observed by other missions (SOHO, SDO, PROBA2);

- To track the connectivity of coronal structures to the solar surface and, in combination with state-of-the-art MHD models, to allow determining reliably on the large-scale coronal magnetic field configuration;
- To investigate the fine structure and dynamics of the corona in that region where energy from eruptive events and magnetic free energy is converted into radiative energy and kinetic energy of plasma motions.

PROBA-3/ASPIICS will perform stereoscopic coronagraphy with Solar Orbiter/Metis and most of the sources of CMEs and solar wind will be measured in situ by Parker Solar Probe and Solar Orbiter. PROBA-3 represents a cornerstone mission for the monitoring and diagnostic of the main solar events and plays a key role in the SW programs.

3.3 HEMERA

HEMERA is a project for the flight of stratospheric balloons with scientific payload, founded by the European Commission, within the Horizon 2020 program, and coordinated by the French space agency CNES. The consortium involves 13 partners from six European countries and Canada. The user community can fly their scientific instrumentation on stratospheric Zero Pressure Balloons (at altitudes of about 35 km) from the range Esrange (Sweden, within the Arctic Polar Circle), or from that of Timmins (Ontario, Canada).

The Solar Physics group of the INAF-OATo is involved in the HEMERA project with the telescope Coronagraph Magnetograph experiment, CorMag, which is an internally occulted 50 mm diameter aperture coronagraph, flying with a zero-pressure stratospheric balloon mission, for the study of the magnetic field topology of the solar corona. CorMag acquires linearly-polarized images of the solar corona, in a 0.5 nm wide band-pass centered on the coronal emission FeXIV at 530.3 nm line, and off-band at 532.3 nm (Fineschi et al. 2021). The CorMag experiment flew for the first time from the Timmins range (Ontario, Canada) on the 17th of August 2022.

This instrument benefits from the heritage of the projects ASPIICS and Antarcticor, the second being its prototype, designed for coronal observations from the Antarctic Italian–French Station Concordia. The scientific activities with the Antarcticor prototype were carried out during two campaigns in Antarctica in 2018/2019 and 2019/2020 (Fineschi et al. 2019). The advantage of observing from high altitudes in the stratosphere, with respect to a classic ground-based coronagraph, is the virtual absence of atmospheric scattering, one of the worst obstacles for the coronal observations from the ground.

The internally occulted coronagraph optical principle is to make an image of the solar disk on an internal occulter, which is a 3.7 mm diameter mirror after the telescope objective lens, which reflects the sun disk light to a trap, leaving the coronal radiation free to pass through a field lens, filter and camera lens assembly, and making an image of the corona on a detector with a linear polarizers mask. The surface brightness of the solar disk is about one million larger than that of the corona, which is our scientific target, hence the most critical parts of the experiment are the blocking of the light from the solar disk and the instrument stray-light suppression. For this purpose, the image of the Sun should be continuously centered in the internal occulter within 1 arcminute of tolerance. Moreover, during the detector exposures, the precision of the tracking must be kept within an accuracy of 10 arcsec, in order to obtain the necessary spatial accuracy in the coronal images.

The telescope is pointed to the Sun by means of an alt-azimuth double fork mount, interfaced with the floor of the balloon gondola, which is suspended to the balloon. During flight, the gondola is subjected to different motions: rotation about its axis of less than 0.1 revolutions per minute, a conical pendulum motion of the flight train of typical frequency 0.05 Hz and amplitude less than 0.1° , a wobbling/oscillation motion around its center of gravity below its attachment point at the flight train, of frequency from 0.5 to 1.0 Hz and amplitude from 0.1° to 0.5° . Therefore, an efficient pointing and tracking system is needed, on both azimuth and elevation angles, aiming to provide the pointing accuracy and stability, which are required by the scientific driver of coronal observation, in order to compensate for the motion of the gondola suspended to the balloon. The gondola itself is provided with an azimuth control system but its relatively low accuracy is not compatible with the pointing and tracking requirements of CorMag. Moreover, the gondola has no control in elevation.

The pointing and tracking system of CorMag is composed of the Sun Sensor Assembly (SSA), which is composed of two sun sensors, one with a large field of view (FoV), $\pm 60^\circ$, and one with a narrow FoV, $\pm 2^\circ$. Two different sensors with different FoVs are required, as a first wide field and relatively coarse sensor is designed to put the Sun in the FoV of the narrow field sensor, having a higher accuracy for the fine tracking. They are basically two pin-hole cameras, making an image of the Sun on a quadrant photodetector device. The incidence angle of the rays from the Sun is measured both in azimuth and elevation, by the induced photocurrents from the four quadrants of the detector, which are converted in azimuthal and elevation angles, and are sent to the control unit of CorMag. The accuracy and the precision of the larger FoV ($\pm 60^\circ$) sensor are respectively better than 0.4° and 0.06° , while the accuracy and the precision of



Fig. 13 The balloon and the gondola with the scientific payload on the runway of the Timmins airport, on the launch morning

the smaller ($\pm 2^\circ$) FoV sensor are respectively better than 0.002° and 0.001° .

Typical temperatures reached by the scientific experiments during the ascent and the float phase, as can be deduced from past balloon missions, range from -55 to $+72^\circ\text{C}$. The operational temperature range of the SSA is between -40 and $+85^\circ\text{C}$, and an external unit will control two heaters to ensure the sensor's survival. The sun sensors will provide information regarding their temperatures in the telemetry (Fig. 13).

The advantages of using pin hole cameras and quadrant detectors, with respect to more traditional optical systems based on the use of lenses and CCD detectors, are that the first type of systems is simpler, hence less prone to failures, and easier to align and calibrate. Their weight is more than one order of magnitude lower than that of a classical telescope for Sun imaging (the weight of a sun sensor is of the order of hundreds of grams), the occupied volume is between 2000 and 3000 mm^3 , and last but not least the analysis of the signal from the detectors does not need elaborated software for image recognition.

The scientific part of the mission will last a 3–6 h. Starting early in the morning, the ascent phase from the Timmins range will take a couple of hours, during which functional tests of the different subsystems will be performed, and just before reaching the float altitude, which typically ranges from 30 to 35 km, the on-flight calibrations will start, by taking images of the Sun through the neutral density filter of the front door, which will be kept closed, until the float altitude will be reached and the actual observations of the corona will start. The float phase will last about 10 h, during which CorMag will alternatively share the observation in the Sun direction with other instruments of the payload. As the telemetry to the ground is limited, allowing only sending

quick look images for calibration and pointing, data will be stored on-board and recovered after the landing. In the descent phase, the gondola will be released, and the parachute will give an acceleration of about 10 g vertically (at the take-off 10 g vertically and 5 g laterally). Hence, for the safety of the instrument and also of the flown over areas, the telescope is properly designed to withstand the resulting mechanical solicitations.

After the CorMag's first flight on August 17, 2022, where the star pointing and tracking system was tested successfully, on August 8, 2023 the coronagraph acquired images of the corona in the polarized emission line of the FeXIV, 530.3 nm. Figure 14 shows the instrument operating at stratospheric altitude during the August 8, 2023 flight.

4 SW enabling science research

4.1 Solar wind with remote-sensing data

The solar wind is a supersonic outflow of completely-ionized plasma which continuously flows from the solar corona into interplanetary space. It is composed of approximately equal numbers of ions and electrons; the ion component consists predominantly of protons (95%) with a contribution of a few percent of alpha particles (doubly ionized helium nuclei) and, much less abundant, heavy ions in different ionization stages.

Different regions of the Sun produce solar wind of different speeds, densities and compositions. Coronal holes produce solar wind of high speed, ranging from 500 to 800 km/s. We suggest to read the reviews about some of the solar wind results obtained by spectroscopic data and summarized by, e.g., Antonucci (2006), Kohl et al. (2006), Abbo et al. (2016), Cranmer et al. (2017) and Cranmer and Winebarger (2019). At solar minimum activity, the north and south poles of the Sun have large, persistent coronal holes, so high latitudes are filled with fast solar wind (see



Fig. 14 CorMag coronagraph on the gondola operating at stratospheric altitude during the August 8, 2023 flight

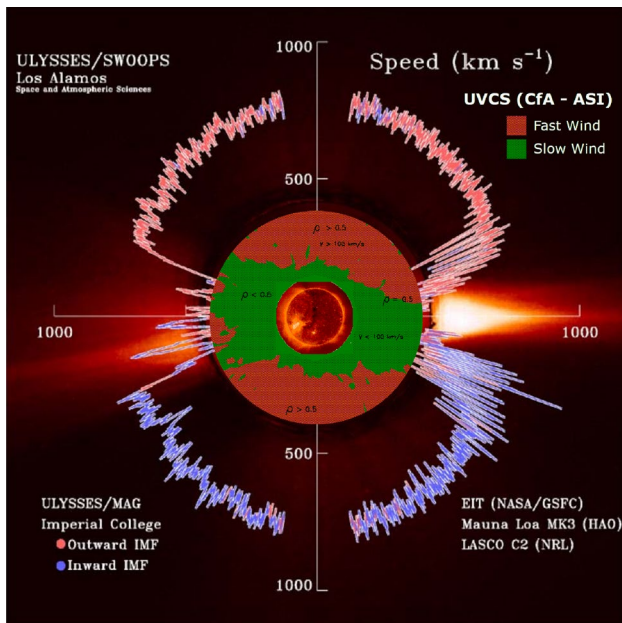


Fig. 15 Solar wind speed and magnetic polarity (red and blue rings) as a function of heliolatitute measured by ESA/NASA deep-space mission Ulysses at large distances from the Sun (≥ 1 AU), overlaid with solar disk image taken with the NASA/GSFC EIT instrument (center) and with the solar corona image taken with NRL LASCO C2 coronagraph (background image) (McComas et al. 1998). In the outer corona, the map of the O VI doublet intensity ratio obtained with UVCS/SOHO instrument represents the slow (green) and fast (red) solar wind as inferred by Doppler dimming diagnostics at the time of the minimum of solar activity (Giordano et al. 1997). The Ulysses speed measurements have been color-coded to indicate the orientation of the observed Interplanetary Magnetic Field: red for outward pointing and blue for inward

Fig. 15). In the equatorial plane, where the Earth and the other planets orbit, the most common state of the solar wind is the slow speed with values of about 400 km/s (e.g., Giordano et al. 1997). In this region is formed the so-called equatorial current sheet, a narrow surface within

the extended solar atmospheres where the magnetic field of the sun changes polarity.

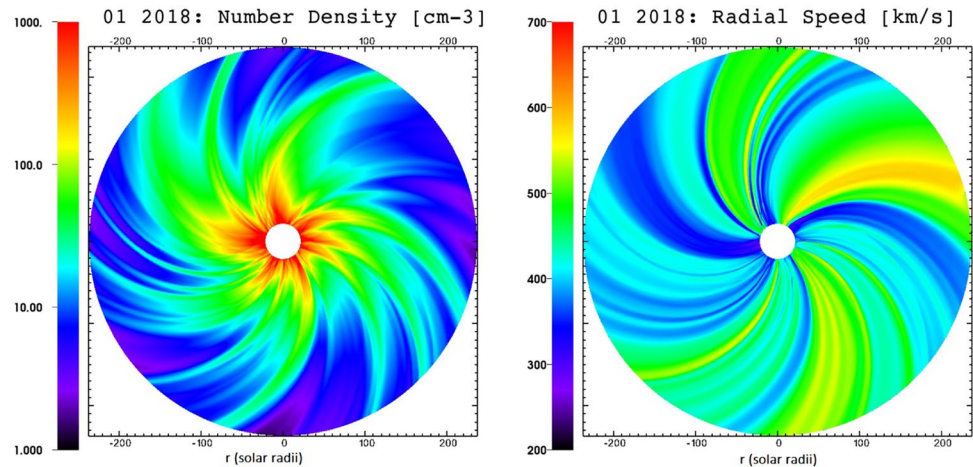
During quiet periods, the current sheet can be nearly flat. As solar activity increases, the solar surface fills with active regions; coronal holes and other complex structures appear even close to the equator, then the structure and speed of the solar wind and the position of the current sheet are modified. Because the Sun rotates every 27 days, the solar wind becomes a complex spiral of high and low speeds and high and low densities that looks like the skirt of a twirling ballerina. When the high-speed solar wind overtakes the slow-speed solar wind, it creates a so-called corotating interaction region. These interaction regions comprise a solar wind with very high densities and strong magnetic fields.

The study of the evolution of the current sheet, the corotating regions, and the position of the Earth with respect to these structures is very important because the transient events of interest for space weather propagate from the Sun to the Earth by interacting with the surrounding medium. SW impacts are highly dependent on the solar wind speed, density, and the direction of the embedded magnetic field.

Each of the elements mentioned above plays a role in SW: in particular, high-speed winds produce geomagnetic storms; corotating interaction regions and, to a lesser extent, current sheet crossings can also cause geomagnetic disturbances. Thus, the study of solar wind characteristics is critical to developing forecasts for SW and its impacts on Earth.

The INAF/OATo group has long experience in determining the speed of the solar wind from various solar structures at different periods of the solar cycle, mainly based on the application of Doppler Dimming diagnostics to UVCS spectroscopic data from SOHO mission (e.g Giordano et al. 1997; Dolei et al. 2018; Bemporad et al. 2021). More recently the data of the Metis instrument, operating on board the Solar Orbiter since 2020, enable to make maps of wind speed in a field of view ranging from 1.5 to over 10 solar radii (Romoli et al. 2021). Moreover, the group is developing

Fig. 16 Pseudocolor plots of the plasma number density (left) and radial speed (right) on the ecliptic plane as obtained with Reverse In situ data and MHD AApproach (RIMAP) from the January 2018 in situ observations (Biondo et al. 2021)



the expertise to reconstruct plasma parameters in interplanetary space based on in situ and low corona observations where the wind is accelerated (see Fig. 16 from Biondo et al. 2021).

4.2 CMEs with remote-sensing data

4.2.1 General introduction

CMEs are energetic events that involve the expulsion of huge amounts of plasma (masses up to 10^{16} g) and magnetic fields into the solar wind, thus representing, together with solar flares, one of the most spectacular examples of explosive energy release from the Sun. Due to the close connection between CMEs and flares, the magnetic reconnection mechanism is supposed to play a major role in CME eruption and evolution. These transient coronal events, whose speeds range from just a few hundred up to 2500 km s^{-1} , are known to drag along the expanding magnetic field, usually in the shape of helical field lines, (i.e. a flux rope), and propagate from the Sun into the heliosphere.

Although CMEs are associated with other energetic solar events, such as flares, eruptive prominences, shocks, EUV waves, their interrelationships are not fully understood as yet, and further work is needed to improve our understanding of these phenomena. As for the flux rope component, we do not know at present whether it is a pre-existing feature (that is, a magnetic flux rope emerging from the sub-photosphere) or it is formed by magnetic reconnection during the eruption itself (Romano et al. 2014).

Nowadays, research on CMEs is very important for both scientific and technological reasons (see e.g., Temmer 2021). In fact, since CMEs transport both plasma and magnetic energy from the solar corona to the heliosphere, they constitute the main cause of extreme SW events. In particular, when CMEs are directed toward the Earth, they can cause huge geomagnetic storms that may affect both our ground- and space-based technology, thus contributing to spacecraft damages, GPS and radio interference, energetic particle radiation (a danger for astronauts or airplane crew), and so on.

In general, CMEs present a tripartite structure (see Fig. 17):

- the **leading edge** represents the foremost expanding bright-front structure. Its characteristics have been attributed to various physical mechanisms. Typical explanations are that the structure is due to either a piston-driven shock wave ahead of the CME or to background magnetic field lines filled with plasma and stored by a compression front. In particular, the arcades of the erupting flux rope may be stretched, with the consequence of the compression of coronal plasma on the outer side of the field line and local increase of density (Chen 2011);

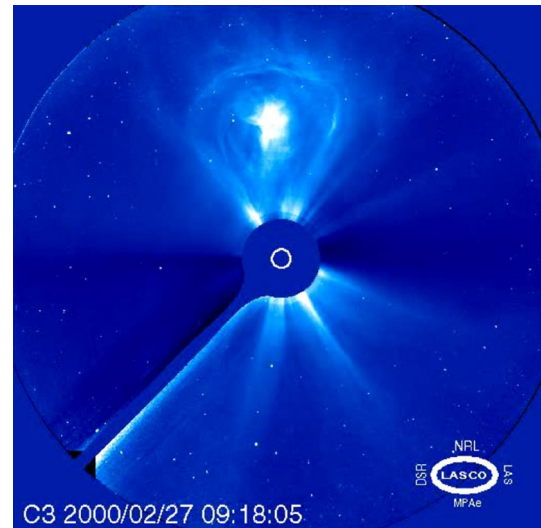


Fig. 17 A typical example of a tripartite CME as seen with a space-based coronagraph, showing the bright core, the dark cavity, and the leading edge

- the **dark cavity**, lying inside the leading edge, is generally interpreted as the expanding flux rope still anchored to the solar surface;
- the **bright core**, surrounded by the cavity, corresponds instead to the eruptive prominence or plasma material expelled from the active region.

4.2.2 Recent research on CMEs carried out in OATo

The INAF-OATo group carried out research on CMEs mostly based on the analysis of data (images and spectra) acquired from space-based observatories, such as SOHO, STEREO, SDO, Hinode, and most recently Solar Orbiter, complemented also with ground-based radiodynamic spectra. The research focused over the last 5 years on many different topics, starting from the studies of CME-driven shock waves combining EUV images of the inner corona and radiodynamic spectra allowing to identify the source of type-II radio burst (Frassati et al. 2019), reconstruct in 3D the shock properties (Mancuso et al. 2019, 2023), measure the jump conditions (compression and heating) across a shock wave (Frassati et al. 2020), report the first unambiguous observational evidence in the radiorange of the reflection of a coronal shock wave at the boundary of a coronal hole (Mancuso et al. 2021), and characterize the statistical properties of the so-called “stealth CMEs” (Ying et al. 2023). Other works combined remote-sensing and in situ data to identify the most probable source of Solar Energetic Particle (SEP) acceleration (Frassati et al. 2022) and study the CME–CME interactions (Telloni et al. 2021).

Physical CME parameters and features can be effectively derived by combining different wavelengths and techniques.

From VL and UV data, it is possible to estimate the temperature and thermal energy evolution of CMEs (Bemporad 2022), studies that required also the previous development of new diagnostic techniques (Ying et al. 2019; Bemporad et al. 2018) based also on numerical modeling (Pagano et al. 2020). Recently, thanks to the availability of data acquired by Solar Orbiter, it was shown that 3D reconstruction of CMEs can be performed by stereoscopic observations employing EUV and VL data (Andretta et al. 2021), and that interesting different morphologies appear in the comparison between VL and UV images (Bemporad et al. 2022) as shown in Fig. 18.

4.3 Solar wind and CMEs with in situ data

In situ measurements acquired by spacecraft in orbit around the Lagrangian point L1 can be fruitfully used to provide short-term, even highly accurate, predictions. Telloni et al. (2019) developed a novel tool to detect and characterize the ICMEs, and to forecast their geo-effectiveness. Specifically, the localization of the ICMEs is enabled by the concurrent identification of the helical properties of the embedded flux rope and an increase in total (thermal plus magnetic) pressure with respect to the unperturbed, pressure-balanced solar wind (Gosling et al. 1994). The energy content of ICMEs is instead used to assess their geo-effectiveness likelihood: only highly energetic ICMEs (either magnetically or kinetically) are indeed likely to transfer a large amount of energy to the Earth's magnetosphere and, therefore, induce geomagnetic disturbances. This tool was tested over a 12-year period and proved to be very reliable in predicting geo-effective

ICMEs (86% (100%) of the weakest (most intense) geomagnetic storms were actually accurately predicted) with an advance warning lying between 2 and 8 h in 98% of the cases.

Telloni et al. (2020) dealt with the relationship existing between solar wind energy and geomagnetic activity. The authors found a clear statistical correlation between the energy carried by the incoming solar wind as measured at L1 and the level of geomagnetic activity, quantified by the Dst-index. This led to the definition of an empirical law for the maximum response of the Earth's magnetosphere to any solar event, which also allows for assessing whether there is no need to provide any alert. Indeed, for very low-energy solar wind plasmas, the empirical relationship predicts a DST remaining above -50 nT, that is, no significant geomagnetic activity. Finally, Telloni et al. (2021) found a relationship to predict the duration of the recovery phase of any geomagnetic event. Specifically, it turned out that the length of the recovery phase depends on the presence of Alfvénic streams following the solar event (either a CME or a CIR) that triggered the geomagnetic disturbance. This piece of information is very important for ground-based technologies and infrastructure that are affected by the integrated effects of geomagnetic disturbances throughout the storm.

The results of the three works cited above and their possible applications to SW science are summarized in Telloni (2022). The aforementioned studies are complemented by the use of deep learning techniques applied to in situ data. This has enabled the delivery of a prediction tool that provides, with 75% reliability, an alert of any geomagnetic event up to 4 h in advance (Telloni et al. 2023). Since the travel

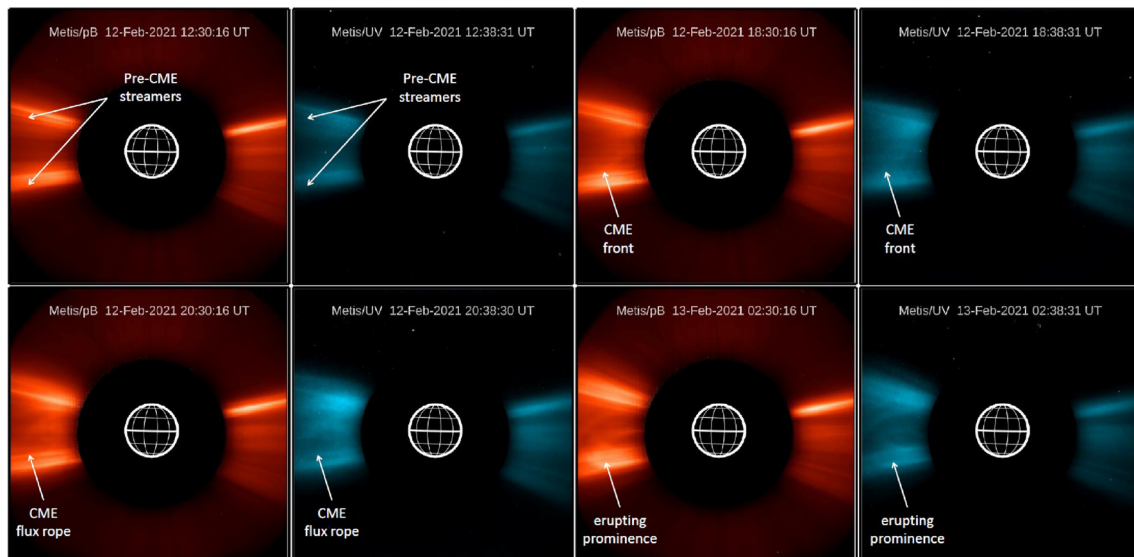


Fig. 18 Example of a CME observed by the Metis coronagraph on-board Solar Orbiter in both VL (red color scale) and UV Lyman- α (light blue color scale) at 4 different times between February 12–13, 2021 (adapted from Bemporad et al. 2022)

time from L1 to Earth of any CME approximately varies from half an hour to an hour, this has also shed light on the time the Earth's magnetosphere needs to respond to a solar event and thus represents a step forward for magnetospheric studies. Indeed, since the difference between the detection of the CME at L1 and the onset of the geomagnetic storm is about 4 h, as statistically evidenced in Telloni et al. (2019) and corroborated by a machine learning approach in Telloni et al. (2023), and the time the CME takes to arrive at Earth is at most 1 h, it turns out that the Earth's magnetosphere takes on average 3 h to get out of equilibrium once hit by a CME. This finding provides thus information on the physics behind the generation of ring currents and the corresponding timescales, opening up wide opportunities for the investigation of these as-yet underexplored topics.

5 Summary

This paper summarized all the main SW projects, SW enabling science projects, and SW enabling science research being currently carried out at the INAF-Turin Astrophysical Observatory (INAF-OATo). Thanks to instrument development and new space mission designs, the provision of new data will significantly improve in the near future our capabilities to monitor solar activity and possibly predict its impact on Earth also with ground-based instruments. At the same time, the availability of these new data has to be coupled with the development of new tools for their automated analysis, and also with the development of new numerical models for the improvement of prediction capabilities. All these skills are present within the solar physics group of INAF-OATo, where they work in synergy providing in the end an improvement in our physical understanding of the complex phenomena governing space weather.

Funding Open access funding provided by Istituto Nazionale di Astrofisica within the CRUI-CARE Agreement.

Data availability All the mentioned data are distributed by the NASA and ESA agencies and can be access and download from the many repositories and archives available on-line. **Open Access** This article is licensed under a Creative Commons Attribution 4.0 International License, which permits use, sharing, adaptation, distribution and reproduction in any medium or format, as long as you give appropriate credit to the original author(s) and the source, provide a link to the Creative Commons licence, and indicate if changes were made. The images or other third party material in this article are included in the article's Creative Commons licence, unless indicated otherwise in a credit line to the material. If material is not included in the article's Creative Commons licence and your intended use is not permitted by statutory regulation or exceeds the permitted use, you will need to obtain permission directly from the copyright holder. To view a copy of this licence, visit <http://creativecommons.org/licenses/by/4.0/>.

References

- Abbo L, Ofman L, Antiochos SK, Hansteen VH, Harra L, Ko Y-K, Lapenta G, Li B, Riley P, Strachan L, von Steiger R, Wang Y-M (2016) Slow solar wind: observations and modeling. *Space Sci Rev* 201(1–4):55–108. <https://doi.org/10.1007/s11214-016-0264-1>
- Andretta V, Bemporad A, De Leo Y, Jerse G, Landini F, Mierla M, Naletto G, Romoli M, Sasso C, Slemmer A, Spadaro D, Susino R, Talpeanu D-C, Telloni D, Teriaca L, Uslenghi M, Antonucci E, Auchère F, Berghmans D, Berlicki A, Capobianco G, Capuano GE, Casini C, Casti M, Chioetto P, Da Deppo V, Fabi M, Fineschi S, Frassati F, Frassetto F, Giordano S, Grimani C, Heinzl P, Liberatore A, Magli E, Massone G, Messerotti M, Moses D, Nicolini G, Pancrazzi M, Pelizzo M-G, Romano P, Schühle U, Stangalini M, Straus T, Volpicelli CA, Zangrilli L, Zuppella P, Abbo L, Aznar Cuadrado R, Bruno R, Ciaravella A, D'Amicis R, Lamy P, Lanzafame A, Malvezzi AM, Nicolosi P, Nisticò G, Peter H, Plainaki C, Poletto L, Reale F, Solanki SK, Strachan L, Tondello G, Tsinganos K, Velli M, Ventura R, Vial J-C, Woch J, Zimbardo G (2021) The first coronal mass ejection observed in both visible-light and UV H I Ly- α channels of the Metis coronagraph on board Solar Orbiter. *Astron Astrophys* 656:14. <https://doi.org/10.1051/0004-6361/202142407>
- Antonucci E (2006) Wind in the solar corona: dynamics and composition. *Sp Sci Rev* 124(1–4):35–50. <https://doi.org/10.1007/s11214-006-9098-6>
- Antonucci E, Romoli M, Andretta V, Fineschi S, Heinzl P, Moses JD, Naletto G, Nicolini G, Spadaro D, Teriaca L, Berlicki A, Capobianco G, Crescenzo G, Da Deppo V, Focardi M, Frassetto F, Heerlein K, Landini F, Magli E, Marco Malvezzi A, Massone G, Melich R, Nicolosi P, Noci G, Pancrazzi M, Pelizzo MG, Poletto L, Sasso C, Schühle U, Solanki SK, Strachan L, Susino R, Tondello G, Uslenghi M, Woch J, Abbo L, Bemporad A, Casti M, Dolei S, Grimani C, Messerotti M, Ricci M, Straus T, Telloni D, Zuppella P, Auchère F, Bruno R, Ciaravella A, Corso AJ, Alvarez Copano M, Aznar Cuadrado R, D'Amicis R, Enge R, Gravina A, Jejičič S, Lamy P, Lanzafame A, Meierdierks T, Papagiannaki I, Peter H, Fernandez Rico G, Giday Sertsu M, Staub J, Tsinganos K, Velli M, Ventura R, Verroi E, Vial J-C, Vives S, Volpicelli A, Werner S, Zerr A, Negri B, Castronuovo M, Gabrielli A, Bertacin R, Carpentiero R, Natalucci S, Marliani F, Cesa M, Laget P, Morea D, Pieraccini S, Radaelli P, Sandri P, Sarra P, Cesare S, Del Forno F, Massa E, Montabone M, Mottini S, Quattropiani D, Schillaci T, Boccardo R, Brando R, Pandi A, Baietto C, Bertone R, Alvarez-Herrero A, García Parejo P, Cebollero M, Amoroso M, Centonze V (2020) Metis: the Solar Orbiter visible light and ultraviolet coronal imager. *Astron Astrophys* 642:10. <https://doi.org/10.1051/0004-6361/201935338>. [arXiv:1911.08462](https://arxiv.org/abs/1911.08462) [astro-ph.SR]
- Bemporad A (2022) Temperature and thermal energy of a coronal mass ejection. *Symmetry* 14(3):468. <https://doi.org/10.3390/sym14030468>
- Bemporad A, Pagano P, Giordano S (2018) Measuring the electron temperatures of coronal mass ejections with future space-based multi-channel coronagraphs: a numerical test. *Astron Astrophys* 619:25. <https://doi.org/10.1051/0004-6361/201833058>
- Bemporad A, Giordano S, Zangrilli L, Frassati F (2021) Combining white light and UV Lyman- α coronagraphic images to determine the solar wind speed. The quick inversion method. *Astron Astrophys* 654:58. <https://doi.org/10.1051/0004-6361/202141276>. [arXiv:2107.06811](https://arxiv.org/abs/2107.06811) [astro-ph.SR]
- Bemporad A, Andretta V, Susino R, Mancuso S, Spadaro D, Mierla M, Berghmans D, D'Huys E, Zhukov AN, Talpeanu D-C, Colaninno R, Hess P, Koza J, Jejičič S, Heinzl P, Antonucci E, Da Deppo V, Fineschi S, Frassati F, Jerse G, Landini F, Naletto G, Nicolini

- G, Pancrazzi M, Romoli M, Sasso C, Slemer A, Stangalini M, Teriaca L (2022) Coronal mass ejection followed by a prominence eruption and a plasma blob as observed by Solar Orbiter. *Astron Astrophys* 665:7. <https://doi.org/10.1051/0004-6361/202243162>. [arXiv:2202.10294](https://arxiv.org/abs/2202.10294) [astro-ph.SR]
- Bemporad A, Abbo L, Barghini D, Benna C, Biondo R, Bonino D, Capobianco G, Carella F, Cora A, Fineschi S, Frassati F, Gardiol D, Giordano S, Liberatore A, Mancuso S, Mignone A, Rasetti S, Reale F, Riva A, Salvati F, Susino R, Volpicelli A, Zangrilli L (2021) SWELTO—Space WEather Laboratory in Turin Observatory. <https://doi.org/10.48550/arXiv.2101.07037>, [arXiv:2101.07037](https://arxiv.org/abs/2101.07037) [astro-ph.SR] (arXiv e-prints)
- Bemporad A, Andretta V, Pancrazzi M, Focardi M, Straus T, Sasso C, Spadaro D, Uslenghi M, Antonucci E, Fineschi S, Abbo L, Nicolini G, Landini F, Romoli M, Naletto G, Nicolosi P (2014) On-board CME detection algorithm for the Solar Orbiter-METIS coronagraph. In: Chiozzi G, Radziwill NM (eds) Software and cyberinfrastructure for astronomy III. Society of Photo-Optical Instrumentation Engineers (SPIE) Conference Series, vol 9152, p 91520. <https://doi.org/10.1117/12.2055511>
- Biondo R, Bemporad A, Mignone A, Reale F (2021) Reconstruction of the Parker spiral with the Reverse In situ data and MHD Approach—RIMAP. *J Sp Weather Sp Clim* 11:7. <https://doi.org/10.1051/swsc/2020072>
- Boni L, Bassetto M, Niccolai L, Mengali G, Quarta AA, Circi C, Pellegrini RC, Cavallini E (2023) Structural response of Helianthus solar sail during attitude maneuvers. *Aerosp Sci Technol* 133:108152. <https://doi.org/10.1016/j.ast.2023.108152>
- Burch JL, Goldstein R, Cravens TE, Gibson WC, Lundin RN, Pollock CJ, Winningham JD, Young DT (2007) RPC-IES: the ion and electron sensor of the Rosetta plasma consortium. *SSR* 128(1–4):697–712. <https://doi.org/10.1007/s11214-006-9002-4>
- Buzulukova N, Tsurutani B (2022) Space weather: from solar origins to risks and hazards evolving in time. *Front Astron Sp Sci* 9:429. <https://doi.org/10.3389/fspas.2022.1017103>. [arXiv:2212.11504](https://arxiv.org/abs/2212.11504) [physics.space-ph]
- Capobianco G, Fineschi S, Massone G, Landini F, Casti M, Bellomo A, Deffacis M, Romoli M, Antonucci E, Andretta V, Naletto G, Nicolini G, Spadaro D (2019) OPSys: optical payload systems facility for space instrumentation integration and calibration. In: International conference on space optics—ICSO 2018. Society of Photo-Optical Instrumentation Engineers (SPIE) Conference Series, vol 11180, p 111807. <https://doi.org/10.1117/12.2536193>
- Carella F, Bemporad A (2020) Automatic identification of EUV structures on the Sun with a Fuzzy clustering algorithm. *INAF Tech Rep* 27:14. <https://doi.org/10.20371/INAF/TechRep/27>
- Carrington RC (1859) Description of a singular appearance seen in the Sun on September 1, 1859. *Mon Not R Astron Soc* 20(1):23–35. <https://doi.org/10.1093/mnras/20.1.13>
- Chandra R, Pariat E, Schmieder B, Mandrini CH, Uddin W (2010) How can a negative magnetic helicity active region generate a positive helicity magnetic cloud? *Sol Phys* 261(1):127–148. <https://doi.org/10.1007/s11207-009-9470-2>. [arXiv:0910.0968](https://arxiv.org/abs/0910.0968) [astro-ph.SR]
- Chen PF (2011) Coronal mass ejections: models and their observational basis. *Liv Rev Sol Phys* 8:1. <https://doi.org/10.12942/lrsp-2011-1>
- Cranmer SR, Winebarger AR (2019) The properties of the solar corona and its connection to the solar wind. *Ann Rev Astron Astrophys* 57:157–187. <https://doi.org/10.1146/annurev-astro-091918-104416>. [arXiv:1811.00461](https://arxiv.org/abs/1811.00461) [astro-ph.SR]
- Cranmer SR, Gibson SE, Riley P (2017) Origins of the ambient solar wind: implications for space weather. *Sp Sci Rev* 212(3–4):1345–1384. <https://doi.org/10.1007/s11214-017-0416-y>. [arXiv:1708.07169](https://arxiv.org/abs/1708.07169) [astro-ph.SR]
- Dasso S (2009) Magnetic helicity content in solar wind flux ropes. In: Gopalswamy N, Webb DF (eds) *Universal heliophysical processes*, vol 257, pp 379–389. <https://doi.org/10.1017/S1743921309029603>
- Dolei S, Susino R, Sasso C, Bemporad A, Andretta V, Spadaro D, Ventura R, Antonucci E, Abbo L, Da Deppo V, Fineschi S, Focardi M, Frassetto F, Giordano S, Landini F, Naletto G, Nicolini G, Nicolosi P, Pancrazzi M, Romoli M, Telloni D (2018) Mapping the solar wind HI outflow velocity in the inner heliosphere by coronagraphic ultraviolet and visible-light observations. *Astron Astrophys* 612:84. <https://doi.org/10.1051/0004-6361/201732118>
- Evans JW (1948) Photometer for measurement of sky brightness near the sun. *J Opt Soc Am* (1917–1983) 38(12):1083
- Fineschi S, Capobianco G, Massone G, Susino R, Zangrilli L, Bemporad A, Liberatore A, Landini F, Romoli M, Damé L, Christille JM, Sandri P, Marmonti M, Galy C (2019) AntarctiCor: solar coronagraph in Antarctica for the ESCAPE project. *Nuovo Cimento C Geophys Sp Phys C* 42(1):26. <https://doi.org/10.1393/ncc/i2019-19026-9>
- Fineschi S, Naletto G, Romoli M, Da Deppo V, Antonucci E, Moses D, Malvezzi AM, Nicolini G, Spadaro D, Teriaca L, Andretta V, Capobianco G, Crescenzo G, Focardi M, Frassetto F, Landini F, Massone G, Melich R, Nicolosi P, Pancrazzi M, Pelizzo MG, Poletto L, Schühle U, Uslenghi M, Vives S, Solanki SK, Heinzel P, Berlicki A, Cesare S, Morea D, Mottini S, Sandri P, Alvarez-Herrero A, Castronuovo M (2020) Optical design of the multi-wavelength imaging coronagraph Metis for the solar orbiter mission. *Exp Astron* 49(3):239–263. <https://doi.org/10.1007/s10686-020-09662-z>
- Fineschi S, Loreggia D, Susino R, Landini F, Romoli M, Capobianco G, Zangrilli L, Liberatore A, Pancrazzi M (2021) The coronal magnetograph (CorMag): deriving the coronal magnetic field topology from Antarctica and the Stratosphere. In: 43rd COSPAR Scientific Assembly. Held 28 January–4 February, vol 43, p 1806
- Frassati F, Susino R, Mancuso S, Bemporad A (2019) Comprehensive analysis of the formation of a shock wave associated with a coronal mass ejection. *Astrophys J* 871(2):212. <https://doi.org/10.3847/1538-4357/aaf9af>
- Frassati F, Mancuso S, Bemporad A (2020) Estimate of plasma temperatures across a CME-driven shock from a comparison between EUV and radio data. *Sol Phys* 295(9):124. <https://doi.org/10.1007/s11207-020-01686-0>
- Frassati F, Laurenza M, Bemporad A, West MJ, Mancuso S, Susino R, Alberti T, Romano P (2022) Acceleration of solar energetic particles through CME-driven shock and streamer interaction. *Astrophys J* 926(2):227. <https://doi.org/10.3847/1538-4357/ac460e>
- Giordano S, Antonucci E, Benna C, Kohl JL, Noci G, Michels J, Fineschi S (1997) Solar wind acceleration in the solar corona. In: Wilson A (ed) *Correlated phenomena at the sun, in the heliosphere and in geospace*, vol 415. ESA Special Publication, p 327
- Gong Q, Socker D (2004) Theoretical study of the occulted solar coronagraph. In: Chen PTC, Fleming JC, Dittman MG (eds) *Optical systems degradation, contamination, and stray light: effects, measurements, and control*. Society of Photo-Optical Instrumentation Engineers (SPIE) Conference Series, vol 5526, pp. 208–219. <https://doi.org/10.1117/12.549275>
- Gosling JT, Bame SJ, McComas DJ, Phillips JL, Scime EE, Pizzo VJ, Goldstein BE, Balogh A (1994) A forward-reverse shock pair in the solar wind driven by over-expansion of a coronal mass ejection: Ulysses observations. *GRL* 21(3):237–240. <https://doi.org/10.1029/94GL00001>
- Hamilton DC, Gloeckler G, Ipavich FM, Stüdemann W, Wilken B, Kremser G (1988) Ring current development during the great geomagnetic storm of February 1986. *J Geophys Res Sp Phys* 93(A12):14343–14355. <https://doi.org/10.1029/JA093iA12p14343>

- Kohl JL, Noci G, Cranmer SR, Raymond JC (2006) Ultraviolet spectroscopy of the extended solar corona. *Astron Astrophys Rev* 13(1–2):31–157. <https://doi.org/10.1007/s00159-005-0026-7>
- Lilensten J, Belhaki A, Messerotti M, Vainio J, Watermann J, Poedts S (2008) EUR 23348—COST action 724—earth system science and management—developing the scientific basis for monitoring, modelling and predicting space weather. COST Office, Office for Official Publications of the European Communities, Luxembourg (ISBN 978-92-898-0044-0)
- Lyot B (1932) Étude de la couronne solaire en dehors des éclipses. Avec 16 figures dans le texte. *Z Astrophys* 5:73
- Mancuso S, Frassati F, Bemporad A, Barghini D (2019) Three-dimensional reconstruction of CME-driven shock-streamer interaction from radio and EUV observations: a different take on the diagnostics of coronal magnetic fields. *Astron Astrophys* 624:2. <https://doi.org/10.1051/0004-6361/201935157>. arXiv:1903.06604 [astro-ph.SR]
- Mancuso S, Bemporad A, Frassati F, Barghini D, Giordano S, Telloni D, Taricco C (2021) Radio evidence for a shock wave reflected by a coronal hole. *Astron Astrophys* 651:14. <https://doi.org/10.1051/0004-6361/202141387>. arXiv:2107.05931 [astro-ph.SR]
- Mancuso S, Barghini D, Bemporad A, Telloni D, Gardiol D, Frassati F, Bizzarri I, Taricco C (2023) Three-dimensional reconstruction of type U radio bursts: a novel remote sensing approach for coronal loops. *Astron Astrophys* 669:28. <https://doi.org/10.1051/0004-6361/202243841>. arXiv:2212.02147 [astro-ph.SR]
- McComas DJ, Bame SJ, Barraclough BL, Feldman WC, Funsten HO, Gosling JT, Riley P, Skoug R, Balogh A, Forsyth R, Goldstein BE, Neugebauer M (1998) Ulysses' return to the slow solar wind. *Geophys Res Lett* 25(1):1–4. <https://doi.org/10.1029/97GL03444>
- Müller D, st. Cyr OC, Zouganelis I, Gilbert HR, Marsden R, Nieves-Chinchilla T, Antonucci E, Auchère F, Berghmans D, Horbury TS, Howard RA, Krucker S, Maksimovic M, Owen CJ, Rochus P, Rodriguez-Pacheco J, Romoli M, Solanki SK, Bruno R, Carlsson M, Fludra A, Harra L, Hassler DM, Livi S, Louarn P, Peter H, Schühle U, Teriaca L, del Toro Iniesta JC, Wimmer-Schweingruber RF, Marsch E, Velli M, De Groof A, Walsh A, Williams D (2020) The solar orbiter mission: science overview. *Astron Astrophys* 642:1. <https://doi.org/10.1051/0004-6361/202038467>. arXiv:2009.00861 [astro-ph.SR]
- Pagano P, Bemporad A, Mackay DH (2020) Hydrogen non-equilibrium ionisation effects in coronal mass ejections. *Astron Astrophys* 637:49. <https://doi.org/10.1051/0004-6361/202037638>. arXiv:2003.12337 [astro-ph.SR]
- Parker EN (1958) Dynamics of the interplanetary gas and magnetic fields. *Astrophys J* 128:664. <https://doi.org/10.1086/146579>
- Plainaki C, Antonucci M, Bemporad A, Berrilli F, Bertucci B, Castonuovo M, De Michelis P, Giardino M, Iuppa R, Laurenza M, Marcucci F, Messerotti M, Narici L, Negri B, Nozzoli F, Orsini S, Romano V, Cavallini E, Polenta G, Ippolito A (2020) Current state and perspectives of Space Weather science in Italy. *J Sp Weather Sp Clim* 10:6. <https://doi.org/10.1051/swsc/2020003>
- Romano P, Zuccarello FP, Guglielmino SL, Zuccarello F (2014) Evolution of the magnetic helicity flux during the formation and eruption of flux ropes. *Astrophys J* 794(2):118. <https://doi.org/10.1088/0004-637X/794/2/118>
- Romoli M, Antonucci E, Andretta V, Capuano GE, Da Deppo V, De Leo Y, Downs C, Fineschi S, Heinzl P, Landini F, Liberatore A, Naletto G, Nicolini G, Pancrazzi M, Sasso C, Spadaro D, Susino R, Telloni D, Teriaca L, Uslenghi M, Wang Y-M, Bemporad A, Capobianco G, Casti M, Fabi M, Frassati F, Frassetto F, Giordano S, Grimani C, Jerse G, Magli E, Massone G, Messerotti M, Moses D, Pelizzo M-G, Romano P, Schühle U, Slemmer A, Stangalini M, Straus T, Volpicelli CA, Zangrilli L, Zuppella P, Abbo L, Auchère F, Aznar Cuadrado R, Berlicki A, Bruno R, Ciaravella A, D'Amicis R, Lamy P, Lanzafame A, Malvezzi AM, Nicolosi P, Nisticò G, Peter H, Plainaki C, Poletto L, Reale F, Solanki SK, Strachan L, Tondello G, Tsinganos K, Velli M, Ventura R, Vial J-C, Woch J, Zimbardo G (2021) First light observations of the solar wind in the outer corona with the Metis coronagraph. *Astron Astrophys* 656:32. <https://doi.org/10.1051/0004-6361/202140980>. arXiv:2106.13344 [astro-ph.SR]
- Telloni D (2022) Statistical methods applied to space weather science. *FrASS* 9:865880. <https://doi.org/10.3389/fspas.2022.865880>
- Telloni D, Bruno R, D'Amicis R, Pietropaolo E, Carbone V (2012) Wavelet analysis as a tool to localize magnetic and cross-helicity events in the solar wind. *Astrophys J* 751(1):19. <https://doi.org/10.1088/0004-637X/751/1/19>
- Telloni D, Perri S, Bruno R, Carbone V, Amicis RD (2013) An analysis of magnetohydrodynamic invariants of magnetic fluctuations within interplanetary flux ropes. *Astrophys J* 776(1):3. <https://doi.org/10.1088/0004-637X/776/1/3>
- Telloni D, Antonucci E, Bemporad A, Bianchi T, Bruno R, Fineschi S, Magli E, Nicolini G, Susino R (2019) Detection of coronal mass ejections at L1 and forecast of their geoeffectiveness. *Astrophys J* 885(2):120. <https://doi.org/10.3847/1538-4357/ab48e9>
- Telloni D, Antonucci E, Bemporad A, Bianchi T, Bruno R, Fineschi S, Magli E, Nicolini G, Susino R (2019) Detection of coronal mass ejections at L1 and forecast of their geoeffectiveness. *ApJ* 885(2):120. <https://doi.org/10.3847/1538-4357/ab48e9>
- Telloni D, Carbone F, Antonucci E, Bruno R, Grimani C, Villante U, Giordano S, Mancuso S, Zangrilli L (2020) Study of the influence of the solar wind energy on the geomagnetic activity for space weather science. *ApJ* 896(2):149. <https://doi.org/10.3847/1538-4357/ab91b9>
- Telloni D, Scolini C, Möstl C, Zank GP, Zhao L-L, Weiss AJ, Reiss MA, Laker R, Perrone D, Khotyaintsev Y, Steinvall K, Sorriso-Valvo L, Horbury TS, Wimmer-Schweingruber RF, Bruno R, D'Amicis R, De Marco R, Jagarlamudi VK, Carbone F, Marino R, Stangalini M, Nakanotani M, Adhikari L, Liang H, Woodham LD, Davies EE, Hietala H, Perri S, Gómez-Herrero R, Rodríguez-Pacheco J, Antonucci E, Romoli M, Fineschi S, Maksimovic M, Souček J, Chust T, Kretschmar M, Vecchio A, Müller D, Zouganelis I, Winslow RM, Giordano S, Mancuso S, Susino R, Ivanovski SL, Messerotti M, O'Brien H, Evans V, Angelini V (2021) Study of two interacting interplanetary coronal mass ejections encountered by Solar Orbiter during its first perihelion passage. Observations and modeling. *Astron Astrophys* 656:5. <https://doi.org/10.1051/0004-6361/202140648>
- Telloni D, D'Amicis R, Bruno R, Perrone D, Sorriso-Valvo L, Raghav AN, Choraghe K (2021) Alfvénicity-related long recovery phases of geomagnetic storms: a space weather perspective. *ApJ* 916(2):64. <https://doi.org/10.3847/1538-4357/ac071f>
- Telloni D, Schiavo ML, Magli E, Fineschi S, Guastavino S, Nicolini G, Susino R, Giordano S, Amadori F, Candiani V, Massone AM, Piana M (2023) Prediction capability of geomagnetic events from solar wind data using neural networks. *Astrophys J* 952(2):111. <https://doi.org/10.3847/1538-4357/acdeea>
- Temmer M (2021) Space weather: the solar perspective. *Liv Rev Sol Phys* 18(1):4. <https://doi.org/10.1007/s41116-021-00030-3>. arXiv:2104.04261 [astro-ph.SR]
- Vourlidas A, Subramanian P, Dere KP, Howard RA (2000) Large-angle spectrometric coronagraph measurements of the energetics of coronal mass ejections. *Astrophys J* 534(1):456–467. <https://doi.org/10.1086/308747>
- Vršnak B, Žic T, Vrbanec D, Temmer M, Rollett T, Möstl C, Veronig A, Čalogović J, Dumbović M, Lulić S, Moon Y-J, Shanmugaraju A (2013) Propagation of interplanetary coronal mass ejections:

- the drag-based model. *Sol Phys* 285(1–2):295–315. <https://doi.org/10.1007/s11207-012-0035-4>
- Ying B, Bemporad A, Giordano S, Pagano P, Feng L, Lu L, Li H, Gan W (2019) First determination of 2D speed distribution within the bodies of coronal mass ejections with cross-correlation analysis. *Astrophys J* 880(1):41. <https://doi.org/10.3847/1538-4357/ab2713>. [arXiv:1905.11772](https://arxiv.org/abs/1905.11772) [astro-ph.SR]
- Ying B, Bemporad A, Feng L, Nitta NV, Gan W (2023) Is there a dynamic difference between stealthy and standard coronal mass ejections? *Astrophys J* 942(1):3. <https://doi.org/10.3847/1538-4357/aca52c>. [arXiv:2211.12825](https://arxiv.org/abs/2211.12825) [astro-ph.SR]
- Zhao XP, Plunkett SP, Liu W (2002) Determination of geometrical and kinematical properties of halo coronal mass ejections using the cone model. *J Geophys Res (Sp Phys)* 107(A8):1223. <https://doi.org/10.1029/2001JA009143>

Publisher's Note Springer Nature remains neutral with regard to jurisdictional claims in published maps and institutional affiliations.